FACULDADE DE ENGENHARIA DA UNIVERSIDADE DO PORTO

Evaluate the Impact of Placing the Vacuum Cup in Distinct Positions During Instrumental Vaginal Delivery

Erica Ferreira

Mestrado em Engenharia Biomédica

Supervisor: Prof. Dulce Oliveira (PhD)

Second Supervisor: Prof. Marco Parente (PhD)

July 18, 2023

Evaluate the Impact of Placing the Vacuum Cup in Distinct Positions During Instrumental Vaginal Delivery

Erica Ferreira

Mestrado em Engenharia Biomédica

July 18, 2023

Abstract

Parturition is a natural and highly complex physiological process that is influenced by the morphology and configuration of the maternal pelvis, as well as uterine contractility and fetal size. In some cases this can be accomplished with the assistance of instruments, like the vacuum-cup, which allows for the reduction of fetal trauma. However, in order for this process to succeed, the vacuum-cup must be correctly positioned. There is currently a defined point of flexion in the fetal head where this instrument should be placed; however, there are various head formats and sizes, and thus the point designated as ideal for a standard head may not be appropriate for a head with a more unusual morphology.

This work had as main objective to study the influence of the vacuum-cup on the pelvic floor of the parturient, namely when used on a head with a different size and shape from the standard heads.

In the first phase, the morphing of several types of heads was performed: where the shape was kept and only the size changed (prematurity, macrocephaly, microcephaly and different percentiles) and where the shape of the head was changed (craniosynostosis: plagiocephaly, scaphocephaly, brachycephaly). After performing the morphing for these situations, their quality was evaluated in order to understand whether the meshes obtained could be used in terms of biomechanical simulations.

To proceed to the biomechanical simulations, the head that mimicked a situation of scaphocephaly was chosen, as it is the craniosynostosis with the highest incidence. Simulations were performed with and without suction cup, and for two different durations of labour: 100 and 150 minutes. The results obtained in relation to the influence of the suction cup showed that, in terms of stress, it has different effects depending on the phase of labour that is being analysed, in terms of stretch there is no influence of the use of this instrument and in terms of reaction forces, for a duration of labour of 100 minutes, these decreased by approximately 61% with the use of the suction cup. With regard to the duration of labour, the results obtained in the simulations with and without suction cup were not in agreement, and in the simulation with suction cup the duration of labour did not result in significant differences in terms of stretch and reaction forces, however, in the simulation without suction cup these two variables varied with time.

Keywords: Biomechanical Simulation, Craniosynostosis, Morphing

Resumo

O parto é um processo natural e fisiológico bastante complexo, que depende da morfologia e configuração da pelve materna, bem como da contratilidade uterina e do tamanho fetal. Em certos casos este pode ser realizado com o auxílio de instrumentos, como é o caso da ventosa, que permite minimizar os traumas no feto. Contudo, de forma a garantir o sucesso deste processo, é necessário que a ventosa seja colocada corretamente. Atualmente, encontra-se definido o ponto de flexão na cabeça fetal onde se deve colocar este instrumento, no entanto, existem diversos formatos e tamanhos de cabeça e, portanto, o ponto tido como ideal para uma cabeça padrão, pode não ser o adequado para uma cabeça com uma morfologia mais incomum.

Assim, este trabalho teve como principal objetivo estudar a influência da ventosa no pavimento pélvico da parturiente, nomeadamente quando utilizada numa cabeça com tamanho e forma diferentes das cabeças padronizadas.

Numa primeira fase foi realizado o *morphing* de diversos tipos de cabeças: em que se mantinha a forma e se alterava apenas o tamanho (prematuridade, macrocefalia, microcefalia e diferentes percentis) e em que se alterava o formato da cabeça (craniossinostoses: plagiocefalia, escafocefalia, braquicefalia). Depois de ter sido realizado o *morphing* para estas situações, foi avaliada a sua qualidade, de forma a perceber se as malhas obtidas poderiam ser utilizadas em termos de simulação biomecânica.

Para prosseguir para as simulações biomecânicas, foi escolhida a cabeça que mimetizava uma situação de escafocefalia, por ser a craniossinostose com maior incidência. Foram realizadas simulações com e sem ventosa, e para duas durações distintas do trabalho de parto: 100 e 150 minutos. Os resultados obtidos em relação à influência da ventosa demonstraram que, em termos de stress esta tem efeitos distintos dependendo da fase do trabalho de parto que esteja a ser analisada, em termos de *stretch* não existe influência do uso deste instrumento e em termos das forças de reação, para uma duração do trabalho de parto de 100 minutos estas diminuiram cerca de 61% com a utilização da ventosa. No que diz respeito à duração do trabalho de parto, os resultados obtidos nas simulações com e sem ventosa não foram concordantes, sendo que na simulação com ventosa o tempo de trabalho de parto não resultou em diferenças significativas em termos de *stretch* e forças de reação, no entanto na simulação sem ventosa estas duas variáveis variaram com o tempo.

Keywords: Craniossinostoses,*Morphing*, Simulação Biomecânica

Acknowledgements

The master's thesis results from the culmination of two years of work and effort, representing the goal of a laborious but rewarding marathon.

As the writer Clarice Lispector states, "those who walk alone may even arrive faster, but the one who goes with someone will certainly go further." And it was for all the accompaniment, help and encouragement that I had, for all those who directly or indirectly accompanied this path, that the realization of this project became possible.

I want to start by thanking INEGI, for making the realization of this project possible.

To Rita and Daniel, I thank all the support they gave me and for always being available to help. Undoubtedly, the time they dedicated to the aid of this project was central to its realization.

To the engineers João Carlos Pereira, Ana Pais and Mariana Carvalho, I thank you for all the time and help you made available to help me in the part of 3D printing.

To my co-advisor, Professor Marco Parente, a thank you for the patience and availability you had in helping me overcome some challenges that were appearing along the way.

To my advisor, Professor Dulce Oliveira, I want to leave a special thanks, for all the availability, support and patience, which, without a doubt, were essential for the realization of this study to be possible. For giving me the possibility and helping to submit my work in the congresses in which I participated, thank you for opening the doors to an endless number of opportunities.

To my parents, family and friends, who always knew how to motivate me to achieve my goals. To Piyush, for the patience, for always saying the right words, for believing in me and never letting me give up.

To all those who made it possible to write a new chapter in the book that illustrates my academic career, my genuine thank you!

Erica Ferreira

"It is the time you have wasted for your rose
That makes your rose so important."

Antoine de Saint-Exupéry

Contents

List of Figures

List of Tables

Abbreviations

AM	Additive Manufacturing
CAD	Computer-Aided Design
CI	Cranial Index
CP	Cephalic Perimeter
CS	Craniosynostosis
CST	Constant Strain Triangle
CVAI	Cranial Vault Asymmetry Index
DBP	Biparietal Diameter
DKT	Discrete Kirchhoff Triangle
DOF	Occipitofrontal Diameter
FDM	Fused Deposition Modelling
FE	Finite Element
FEM	Finite Element Method
IVD	Instrumental Vaginal Delivery
MMI	Modified Moulding Index
MRI	Magnetic Resonance Imaging
PFM	Pelvic Floor Muscle
PI	Plagiocephaly Index
PLA	Polylactic Acid
RBF	Radial Basis Function
SC	Scaphocephaly

Chapter 1

Introduction

This chapter presents a contextualization related to childbirth, specifically instrumented vaginal delivery, as well as the motivation and main objectives of this project.

1.1 Background and Motivation

Childbirth is a complex natural and physiological process, and should always be carried out in the safest way possible [1].

Annually, around 2,7 million babies worldwide die as newborns and more than 300 000 mothers die from childbirth-related complications [2]. One of the most important causes of maternal and perinatal morbidity and mortality in low- and middle-income countries is the prolonged second stage of childbirth. The interventions that aim to put an end in the second prolonged phase of childbirth are instrumented vaginal delivery (IVD) and cesarean section. IVD has several advantages over cesarean section, including avoiding anaesthesia-related risks and reducing the risks of surgery-related bleeding and infections [3]. In addition to termination of the prolonged second stage of labor (when the delivery time exceeds the 180 minutes [4]), IVD is used when immediate delivery or potential fetal compromise is suspected [5].

IVD then refers to the use of an instrument (vacuum-cup or forceps) to assist fetal extraction. The vacuum-cup tends to be the instrument of choice, as can be seen in the graph shown in figure 1.1, since the traction force it exerts on the fetal head is substantially lower than that exerted by forceps, making the fetus safer and reducing the probability of maternal morbidity [5, 6]. Besides that, learning how to use a vacuum-cup seems quicker than a forceps, however the time from decision to extraction is longer than with forceps. In cases of low presentation with transverse or posterior variety or when no analgesia is available, a vacuum extractor is advised. Forceps are more effective than suction, and are suggested in cases of preterm and total anesthesia. Immediate maternal problems (cervical tear, vaginal and perineal laceration, episiotomy use) are less common when using a vacuum-cup. Long-term effects on the pelvic floor and bladder continence for both

forceps and vacuum are equivalent to normal delivery, although anal incontinence is enhanced, particularly with forceps. Both instruments have comparable benign acute neonatal morbidity, however there are some particular problems . Thus, cephalhaematomas and potentially dramatic widespread subgaleal haematomas (rarely), retinal bleeding are possible [7].

IVD is more prevalent in high-income countries, with rates of IVD use in Australia, Canada, Ireland, the Netherlands, Scotland and England ranging from 10% to 16%. Although reliable global statistics on IVD are not available, there is clear evidence that the number of cesarean sections is increasing, reaching epidemic proportions in some countries [5, 8]. Although the rates of IVD are decreasing, the obstetric vacuuum-cup has re-emerged as one of the preferred methods in the instrumentation of labor. However, there are situations in which the use of the vacuum-cup is not recommended because it increases the risk of fetal morbidity. Furthermore, there are several complications arising from the use of the vacuum-cup, both for the mother and the fetus. For the parturient, the short-term risks of instrumented delivery include perineal pain at delivery and in the immediate postpartum period, lacerations and haematomas of the lower genital tract, urinary retention and incontinence, anaemia and faecal incontinence, which may lead to re-hospitalization. Although these risks also exist in spontaneous delivery that does not require instrument-assisted delivery, they are often more associated with IVD. With regard to neonatal complications, it is estimated that the risk of these is around 5%, with serious complications being rare [9].

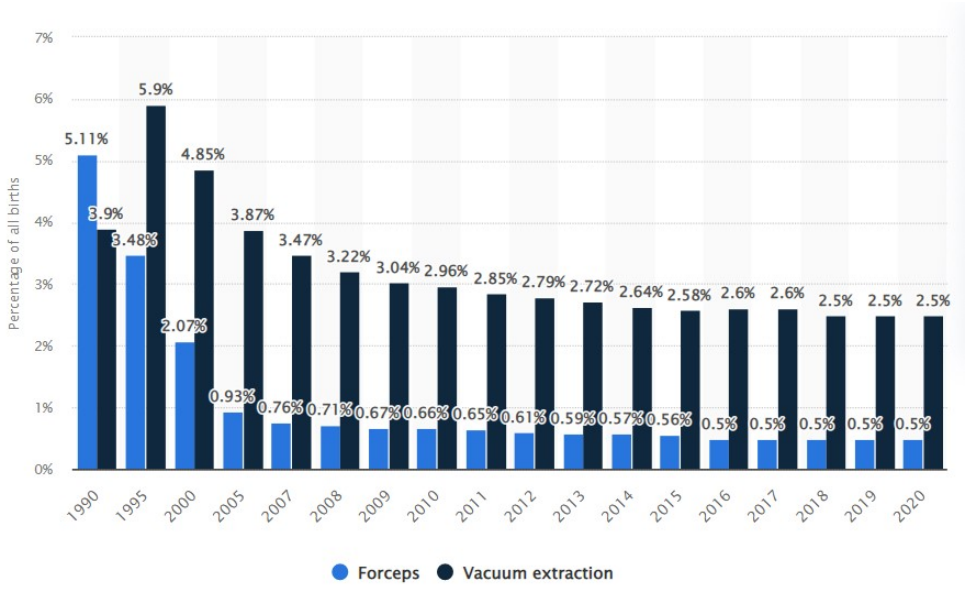

Figure 1.1: Percentage of births by forceps or vacuum-cups in the United States from 1990 to 2020 (retrieved from [10]).

1.2 Aim

The main objective of the dissertation is to evaluate the influence of the use of the vacuum-cup in childbirth, namely in terms of the injuries suffered by the maternal pelvis. Thus, it is necessary

to mimic the aspiration mechanism that occurs between the fetal head and the vacuum-up. This work includes the exploration of several tools related to the performance of finite element (FE) simulations in Abaqus software.

This project's main target audience is obstetricians who, with this study, have a better understanding of the effects of the vacuum-cup, especially when used on non-standard heads. In addition to the effects, they can obtain the necessary information to know which changes to adopt in the methodology currently used, namely the vacuum-cup insertion point, in cases where the foetuses do not have standard heads.

To achieve the objectives proposed for this study, firstly, it was performed the morphing of several head shapes, symmetrical and asymmetrical. In a second phase, the biomechanical simulation of birth with and without vacuum-cup was performed, for an asymmetric head obtained through the previously performed morphing.

With this work, it is expected to obtain a better understanding of the influence of the obstetric vacuum-cup in instrumented vaginal delivery, especially regarding its use when there are heads with unusual morphology. Thus, in practical terms, this would contribute to a better use of this instrument, emphasising in which situations it should or should not be used, and which is the correct way to use it for each case. Thus, with the modelling of the anomalies, it will be possible to give indications about the position of the vacuum-cup, specifically if the position adopted for a common morphology can also be used in cases where the anomalies under study are found.

1.3 Structure of the Dissertation

In addition to the introduction, this dissertation contains 6 more chapters. In the chapter 2, the basic concepts necessary to understand the study undertaken are presented. These include the anatomy of the maternal pelvis and fetal head and the mechanisms of childbirth. In addition, instrumented vaginal delivery is briefly presented, with a focus on vacuum-cup delivery. Finally, the conditions affecting head shape that will be the target of this study are presented. In chapter 3, the state of the art is described and related papers are presented. In chapter 4, the performed morphing of the various fetal heads is presented. In chapter 5 the simulations performed and the results of these simulations are described and a brief discussion of these results is presented. In the chapter 6 the additive manufacturing technique chosen to perform the printing of the heads is explained. In the chapter 7 the main conclusions and future perspectives are presented. Finally, the annexes (A) present the abstracts of this project submitted to the CNB, the IJUP and the ESB, as well as the article submitted for publication in a book of CNB papers in Springer's book series "Lecture Notes in Bioengineering".

Chapter 2

Childbirth

The world is a dynamic system, yet it is not always easy to understand, without further processing, the processes that occur in nature. Either by its complexity or by the lack of processing capacity of the human brain, certain processes are difficult, if not impossible, to simulate only in the mind. Thus, the use of computation and simulation techniques becomes essential to better explain and understand certain systems and their inherent dynamics [11]. Furthermore, these methods make it possible to overcome various ethical and technical issues that arise when these studies are to be carried out *in vivo* [12]. One of the most used computational methods and that has proven to be a powerful tool in engineering is the Finite Element Method (FEM), which allows the mechanical behaviour of mechanical systems, physical structures and, more recently, biological processes to be analysed [13].

2.1 Introduction

Birth is, in the vast majority of cases, a natural and physiological process, yet quite complex. Childbirth can be defined as the sequence of events that result in the termination of pregnancy and the expulsion of the fetus and placenta through the vaginal canal. It begins with involuntary uterine contractions, which, combined with voluntary exertion of the abdominal wall, result in the expulsion of the products of conception through the vaginal canal. The fetal presentation (part of the fetal body that exits first through the vaginal canal) needs to adapt to the smallest possible diameters of the maternal pelvis in order to transpose the most favourable dimensions and contours that are achieved during the course of labor. Thus, the birth process is dependent on the morphology and structure of the maternal pelvis, as well as uterine contractility and fetal size. [1, 14].

2.2 Maternal Pelvis

The pelvis, shown in figure 2.1a corresponds to the compartment surrounded by the pelvic girdle (bony pelvis), part of the appendicular skeleton of the lower limb [15]. The female pelvis has essential functions such as aiding human locomotion and the support of abdominal organs by the pelvic floor muscles (PFM) and the pelvis itself. It also has a central role in childbirth, since the fetus needs to pass through the birth canal, composed of the uterus, cervix, vagina and vulva, which correspond to structures present in the pelvic girdle [12]. It is generally divided into 2

regions: the major (or false) pelvis, which consists essentially of the space above the iliopectineal line, including the two iliac fossae and the region between them, and the minor (or true) pelvis, which lies below the iliopectineal line and is bounded anteriorly by the pubic bones, posteriorly by the sacrum and coccyx, and laterally by the ischium and a small segment of the ilium. [12, 15]. The lesser pelvis creates the pathway during childbirth and is therefore the most important part of the obstetric area [12].

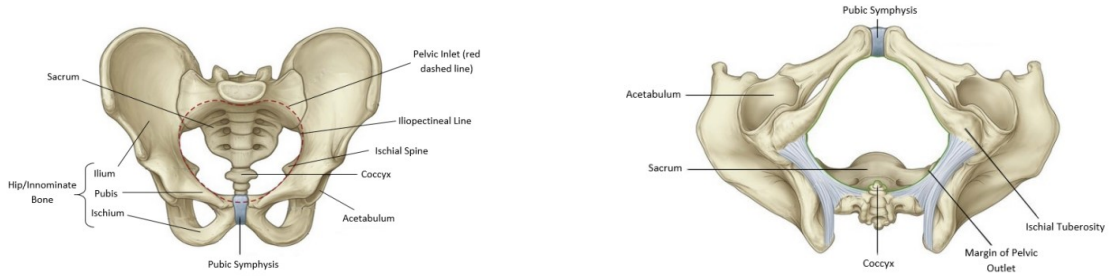

(a) Anterior view of the pelvis.

(b) Pelvic outlet

Figure 2.1: Maternal Pelvis (retrieved from [12]).

The pelvic ligaments soften in the final months of pregnancy and during labor, allowing the sacrococcygeal joint to move and the coccyx to rotate. A typical coccyx can rotate between 5 and 22 degrees; however, with an instrumented vaginal birth, the coccyx can rotate more than 22 degrees, resulting in fracture. [12, 15].

2.3 Fetal Head

The fetal skull is composed of 5 bones: two frontal bones, two parietal bones and an occipital bone [12]. The skull of a newborn baby is made up of bones and sutures that make it malleable to allow it to pass through the birth canal at birth, and to accommodate and expand the encephalon [16, 17]. Indeed, during the first years of life, the brain is in a phase of rapid growth, quadrupling in volume during the first two years of life [16, 18].

The skull is then composed of four primary sutures (metopic, sagittal, coronal and lambdoid), three secondary sutures (frontonasal, scalamus temporal and frontoesphenoid), four fontanelles (posterior, anterior, sphenoid and mastoid) and four main bones (frontal, temporal, parietal and occipital), as represented in the figure 2.2.

During vaginal delivery, the fetal head molds itself into an elongated shape in order to adapt to the birth canal. This process is called molding of the fetal head and is the result of external compressive forces (i.e. the pressure exerted when the fetus is expelled). This molding mechanism is due to the presence of sutures and fontanelles and to the elastic behavior of the bones of the skull, which have the ability to move in relation to each other and to overlap. However, in some cases excessive molding may occur due to prolonged labor or forceful contractions, which can result in various problems in the fetal head such as bone lesions and intracranial hypertension [1].

2.4 Physiological Preparation for Childbirth

Usually several physiological preparatory changes occur before the onset of labor. In early pregnancies, the positioning of the fetal head at the edge of the pelvis usually occurs at least 2 weeks

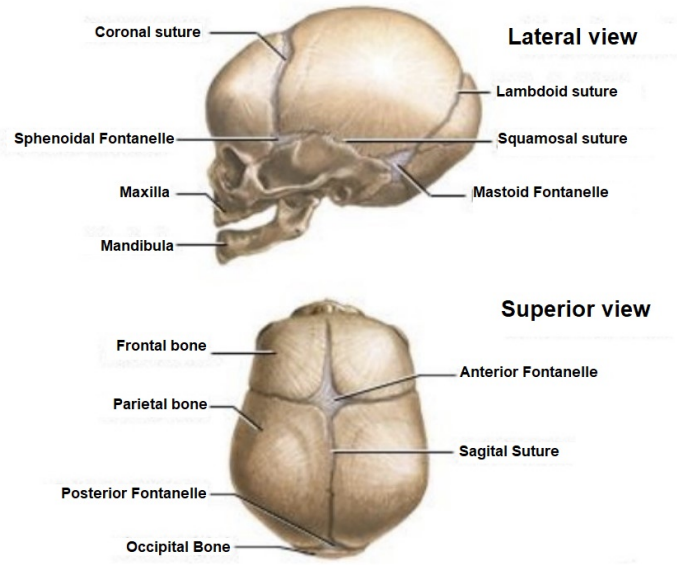

Figure 2.2: Geometry of the skull, sutures and fontanelles of a newborn baby (adapted from [19]).

before the birth, while in the case of women who have previously had a birth, this often does not occur until the start of labor [15].

During the last 4 to 8 weeks of pregnancy, irregular uterine contractions occur, usually painless and with a slowly increasing frequency: Braxton-Hicks contractions [12].

Over the course of several days to several weeks before the onset of labor, the cervix begins to soften and dilate, and in many cases by the time labor starts, it is already dilated by about 1 to 3 cm in diameter [12, 15].

2.5 Mechanisms of normal childbirth

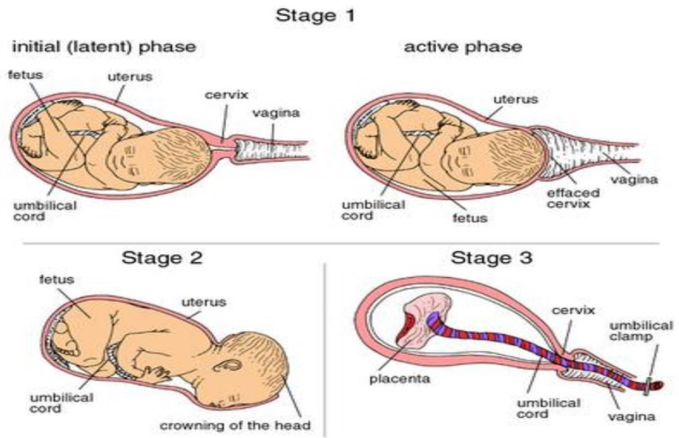

Figure 2.3: Stages of labor (adapted from [20]).

Fetal birth includes the period from the beginning of regular contractions to the expulsion of the placenta, and normal labor is a continuous process divided into 3 stages: the first stage is the interval between the beginning of labor and cervical dilation; the second is the interval between full cervical dilation and expulsion of the fetus; and the third is the interval between expulsion of the fetus and the placental expulsion, as shown in the figure 2.3 [12, 15].

The birth mechanism follows the "theory of least resistance" as the fetal presentation needs to adapt to the smallest possible diameters in order to transpose the most favourable dimensions and contours that are reached during the birth path [13]. Therefore, this mechanism depends on the complex interaction between three variables: uterine activity, the fetus and the maternal pelvis [12, 15].

The frequency, amplitude (strength), and duration of contractions define uterine activity. These contractions are necessary in vaginal birth because, in an efficient vaginal delivery, the fetal head descends as the cervix dilates, and this requires a proper pattern of uterine contractions. Otherwise, scalp edema or fetal head molding with overlapping skull bones may ensue. [12, 15].

With regard to the fetus, there are several variables that influence the delivery mechanism: fetal size, orientation, fetal presentation (fetal part that directly overlaps the pelvic inlet), the "attitude" (*lie*-the degree of flexion and/or extension of the fetal head - figure 2.4; flexion of the head is important to facilitate involvement of the head in the maternal pelvis), position (refers to the relationship of fetal presentation to the maternal pelvis-figure 2.5, and for cephalic presentations, the reference position is the occipitofrontal one) and the "station" (measure of descent of the bony part of the fetal presentation through the birth canal) [12, 15].

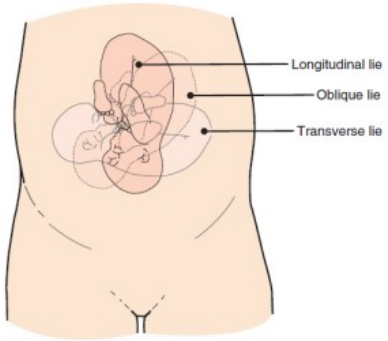

Figure 2.4: Examples of fetal "attitude" (retrieved from [12]).

The mechanisms of breech birth, usually called cardinal movements, correspond to the changes in the position of the fetal head during its passage through the birth canal. These rotations are necessary for the fetus to pass through the birth canal due to the asymmetry of both the fetal head and maternal pelvis. Although birth is a continuous process, there are 7 discrete cardinal movements of the fetus: engagement, descent, flexion, internal rotation, extension, external rotation or restitution, and expulsion, as shown in the figure 2.6 [13].

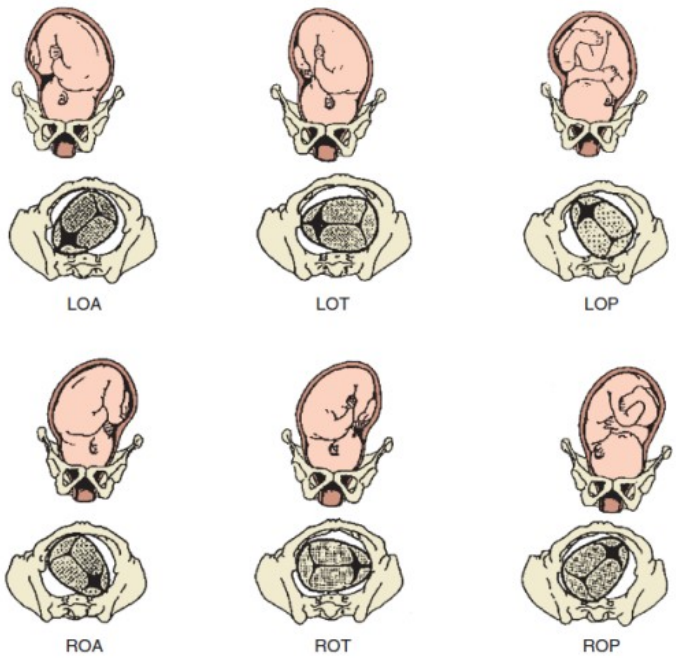

Figure 2.5: Fetal presentation and position. LOA: left anterior occipital; LOT: transverse left occipital; LOP: left posterior occipital; ROA: right anterior occipital; ROT: transverse right occipital; ROP: right posterior occipital (retrieved from [12]).

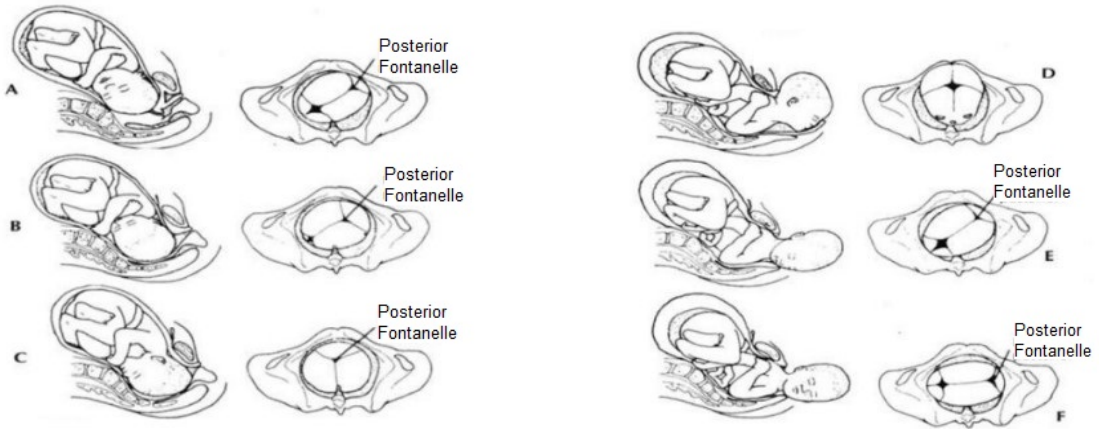

Figure 2.6: Mechanism of delivery in anterior left occipito-iliac presentation (adapted from [13]).

2.6 Instrumented Delivery

In some cases an instrumented vaginal delivery can be performed, using forceps or a vacuum-cup, which are represented in the figure 2.7, as birth aids. The forceps is a metal instrument composed of two spoons, with each half having a curvature that fits around the head of the fetus, allowing it to be pulled out. In turn, the vacuum-cup (also known as suction cup or vacuum extractor) is shaped like a cup, which can be rigid or malleable, that is placed on the fetal head, and a negative

suction pressure is generated between the suction cup bell and the fetal presentation, which allows adaptation between the two and ultimately assists in the expulsion of the fetus. The use of either instrument carries risks for both the mother and the fetus, the main ones being: lacerations of the genital area and pain or injury to the perineum (tissue between the vagina and anus) for the first intervening party, and small injuries to the face for the second. Generally, the vacuum-cup presents less risk of injury for both the mother and the fetus, and is therefore considered safer, as it minimises trauma [13, 21].

(a) Forceps (b) Vacuum-cup

Figure 2.7: Instruments that can be used in the birth aid.

The correct placement of the vacuum-cup is fundamental to ensure the success of this process, and for this it is necessary to correctly identify the flexion point on the fetal head, as shown in figure 2.8 [13].

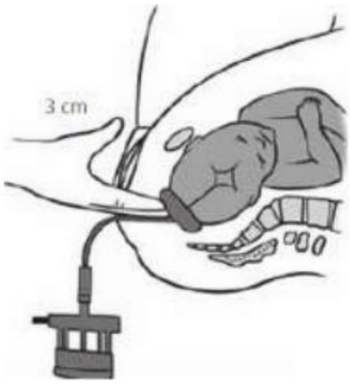

Figure 2.8: Vacuum-cup insertion (retrieved from [13]).

However, there are different head shapes and sizes, which may influence the success of this process. The Portuguese General Direction of Health has published a Normative Circular where it presents the percentage curves for several growth parameters, among which the cephalic perimeter (CP). These data can be found in table 2.1 [22].

Table 2.1: Values of the Cephalic Perimeter according to gender and percentile [22].

Percentile	Cephalic perimeter female gender (cm)	Cephalic perimeter masculine gender (cm)
95	37,5	38,5
90	37	38
75	36	37
50	35	36
25	34	34,5
10	33	33
5	32,5	37,5

As previously mentioned, serious complications are rare, since the systematic performance of ultrasound and radiography allows the diagnosis of many complications that do not present symptoms. However, almost all newborns will present visible effects on the fetal scalp where the vacuum-cup was applied, and these may be of variable degree. Most are transient and of no great clinical importance. In addition, it is estimated that there is an incidence of lacerations of the fetal scalp of about 11%, and this may vary between 1% and 82%, however, these are usually superficial and small. Another consequence that occurs with an incidence varying between 10% and 25% is the cephalohematoma, which consists of the accumulation of serosanguinous fluid under the periosteum of the bones of the skull, as a consequence of the rupture of vessels between the skull and the periosteum. However, the clinical significance of cephalohematoma is minimal because, given that blood is confined to the limits of the periosteum, the amount of blood that can accumulate in this potential space is limited. Nevertheless, there are situations in which a subgaleal haemorrhage may occur and, in this case, as the suture lines do not limit the potential space, the newborn may lose up to about 80% of its blood volume into this space. This complication has an incidence of about 1-4% in deliveries instrumented by vacuum-cup and a mortality rate that may reach 25% if left untreated. In terms of haemorrhages, intracranial haemorrhages and retinal haemorrhages may also occur, the former having an incidence of about 5-6/10,000 live births and may be potentially fatal or cause long-term disability. In turn, the latter is usually transient and there is no evidence that it results in long-term consequences, either developmental or ophthalmological. Finally, skull fractures and neonatal jaundice, and, more rarely, encephalocele may also occur [9].

It is therefore necessary to study the influence of the vacuum-cup on different types of heads to understand its impact, since, as can be seen in the figure 2.9, its suction effect can cause harmful effects if it is not correctly positioned [13].

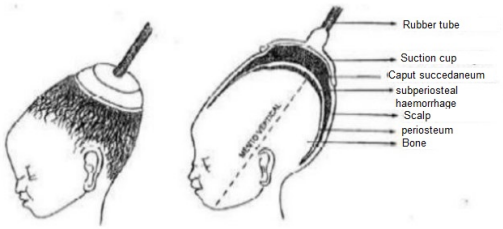

Figure 2.9: Vacuum-cup effects (retrieved from [13]).

2.7 Conditions affecting head size

There are several conditions that affect head size, causing it to be either smaller or larger than expected, which influences the success of instrumented cup delivery.

2.7.1 Prematurity

A fetus is considered premature when born before 37 weeks of gestation, and is considered high-risk premature when born before 32 weeks of pregnancy or weighing less than 1500 g [23]. Studies indicate that the CP of a newborn baby who is not born prematurely is between 33 and 36 cm [24, 25, 26]. A study carried out in Mexico concluded that the average head circumference of fetuses born prematurely is approximately 25,9 cm [27].

2.7.2 Microcephaly

Microcephaly is the reduction of the brain capacity, which can be divided into primary microcephaly, in which the brain does not reach the desired size during pregnancy, and secondary microcephaly, which occurs when the fetus is born with a head of the expected size, but later does not grow as expected. [28]. Generally, in these cases the CP value is less than 31,9 cm [29].

2.7.3 Macrocephaly

Macrocephaly, as opposed to microcephaly, corresponds to an increase in CP, generally above the 97th percentile stipulated for the gestational age and gender of the fetus. When it is higher than 60,0 cm, we are faced with extreme macrocephaly [29, 30].

2.8 Conditions affecting head shape: Craniosynostosis

The sutures and fontanelles play a central role in childbirth, allowing the moulding of the foetal head. 2.2.

Table 2.2: Age of fusion/closure of sutures and fontanelles (retrieved from [17]).

Structure	Average Closure Age
Posterior Fontanelle	3 months
Metopic suture	9-11 months
Anterior Fontanelle	24 months
Sphenoidal Fontanelles	6-24 months
Mastoid Fontanelles	6-24 months
Sagital Suture	30-40 years
Coronal sutures	30-40 years
Lambdoid sutures	30-40 years
Squamous Sutures	30-40 years

When there is a premature fusion of one or more cranial sutures we are faced with craniosynostosis (CS). This type of congenital malformation has an incidence of around 1:2000 live births and a prevalence of 14,1:10 000, resulting in a cranial or craniofacial deformity, as there is a restriction in the development of part of the skull, which is compensated for by abnormal growth in other areas [17, 16, 31, 32]. This is associated with functional problems such as cranial hypertension, cerebral, ocular and neuropsychic lesions, and generally these functional problems tend to increase with the number of sutures affected [17].

There are several classifications for CS, as can be seen in the scheme presented in figure 2.10.

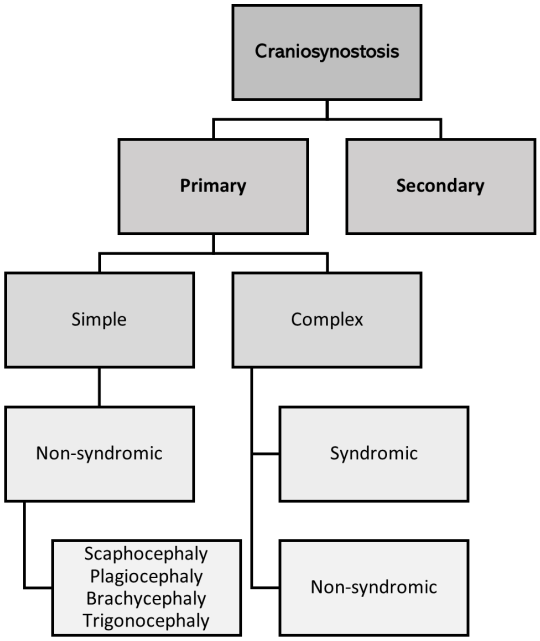

Figure 2.10: Classification of the CS.

Primary CS results from genetic and environmental influences, i.e., early closure of the sutures occurs due to intrinsic alterations of the sutures themselves, without modification of the cerebral growth potential, while secondary CS may result from metabolic disorders, several malformations, among others. Primary CS conditions changes in skull morphology without significant modification of its perimeter, and may be simple, involving a single suture, or complex, involving two or more sutures, which, in turn, may be syndromic, if associated with facial and sometimes extracranial malformations, or non-syndromic [17, 16, 32]. However, the classification that is most commonly used is based on the suture that closed early, and we may have: scaphocephaly if there was early closure of the sagittal suture, trigonocephaly in the case of metopic suture, plagiocephaly in the case of unilateral closure of either the coronal suture or the lambdoid suture and finally brachycephaly, in the case of early closure of the coronal and/or lambdoid sutures. [32]. These are represented in figure 2.11. It should be noted that a child may present up to two deformities at the same time [18]. The shape adopted by the skull depends on the suture involved, the restricted elements and the compensatory elements [17].

Simple, primary, non-syndromic CS are the most frequent type of CS, representing approximately 90% of the recorded cases. The etiological factors that cause the early closure of sutures in these cases are unknown, but some risk factors have already been identified, including biomechanical, environmental and genetic factors. Bearing in mind the purpose of the present project, the relevance of biomechanical factors stands out, since studies indicate that abnormal pressure on the skull that is still developing may cause fusion of the sutures, and this abnormal pressure may result from a pelvic presentation of the fetus, in which its skull is pressed by the maternal ribs, or even from a twin pregnancy [17].

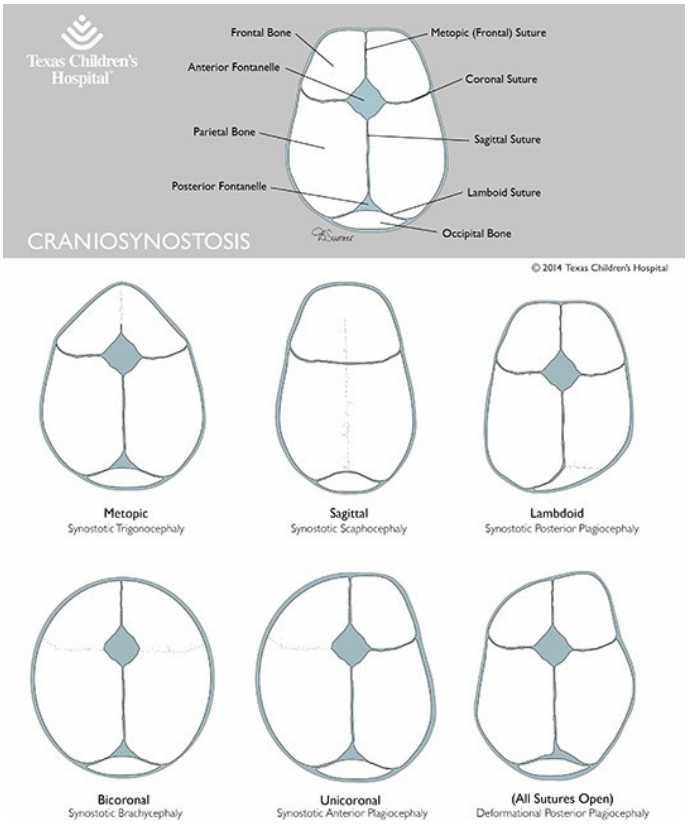

Figure 2.11: Craniosynostosis and related sutures (retrieved from [33]).

2.8.1 Scaphocephaly

Scaphycephaly (SC), also known as dolicephaly, is the most frequent type of CS, responsible for approximately 40% to 60% of cases. This is a consequence of the early closure of the sagittal suture and is not associated with syndromes, resulting in an increase in skull length and reduction in skull width, as represented in figure 2.11. The skull thus becomes elongated, and there may be a predominance of frontal or occipital growth, commonly known as hump or projection, and a syndromic thinning or frontal enlargement may also occur. [17, 16, 18, 32]. In terms of other malformations which may be associated, although rare, studies indicate that heart problems can be diagnosed in 4% of cases, cranial hypertension in 17% and mental retardation in 2,4%. In addition to this, there is also an increase in CP [17].

As regards the diagnosis of SC, the cranial index (CI) is usually used, also known as the cephalic index, which relates the length and width of the skull, these being given by the occipitofrontal diameter (DOF) and biparietal diameter (BPD) respectively, related as shown in the equation 2.1 [18, 32].

$$IC = \frac{DBP}{DOF} * 100 \tag{2.1}$$

In the literature, the range of values considered as normal varies from author to author, with some stating that these are between 76% and 78%, with children with CS presenting a CI varying between 60% and 67%. [32]. Others, as can be seen in the figure 2.12, present a scale of severity for both scaphycephaly and brachycephaly.

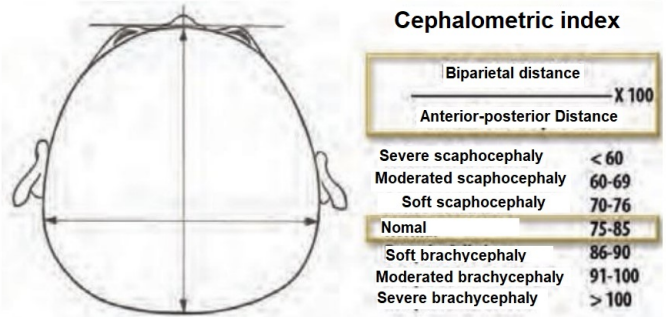

Figure 2.12: Cephalometric index calculation (adapted from [34]).

2.8.2 Trigonocephaly

Trigonocephaly is a congenital deformity of the skull resulting from premature fusion of the metopic suture (before the 3rd month) and is characterized by a triangular and pointed frontal bone due to the restriction of the transverse growth of the frontal bones. In more severe cases there may be restriction of the expansion of the anterior fossa, resulting in hypotelorbitism and reduction of cranial volume and consequently trigonocephaly. It should be noted that the internal distance between the corners of the eyes (internal intercanthal distance) is considered normal when its average is between 2 and 2,5 cm in the first year of life, this being a good parameter to evaluate this CS. This comprises 10 to 31% of all isolated cases of CS, being the second most common type of CS [17, 16, 32, 35, 36, 37].

Usually trigonocephaly is non-syndromic, however there are reports of some cases in which it may be associated with a syndrome, with syndromic forms constituting only 5,5% of cases [17, 36].

Metopic CS is the only sutural synostosis that can be associated with cognitive disorders, mainly due to restricted frontal lobe growth [16]. In fact, between 8% and 33% of patients with trigonocephaly have high intracranial pressure, which may result in delays in the neurodevelopment of the child. Furthermore, between 6% and 10% of patients with this CS present genetic alterations [36].

2.8.3 Plagiocephaly

Plagiocephaly results from the early closure of one of the coronal sutures, leading to craniofacial asymmetry, generally characterised by oblique head asymmetry. [18, 32]. This may be anterior - unilateral coronal synostosis - or posterior - unilateral lambdoid synostosis [38], where unilateral coronal synostoses correspond to about 20% of synostoses, affecting 40/10000 children [17] and, in turn, lambdoid synostosis corresponds to about 1-2% of cases of craniosynostosis [39].

Lambdoid synostosis is clinically distinguished from coronal synostosis by the sparse involvement of the orbital, nasal and mandibular regions [39]. Early fusion of the coronal suture leads to a flattening of the frontal bone and ipsilateral orbital to the site of fusion, and studies indicate that about 50-60% of children with this synostosis have strabismus [16]. This dysmorphism tends to worsen with time and, besides leading to oculomotor and refractive alterations, it also leads to postural problems. Thus, it constitutes the most complex craniofacial deformity among the isolated, simple and non-syndromic synostoses [17].

With regard to diagnosis, the cranial vault asymmetry index (CVAI) is used, obtained mathematically using the equation 2.2.

$$CVAI(\%) = \frac{BiggerDiagonal - SmallerDiagonal}{BiggerDiagonal} * 100 \quad (2.2)$$

The diagonals to which the equation refers are shown in the figure 2.13.

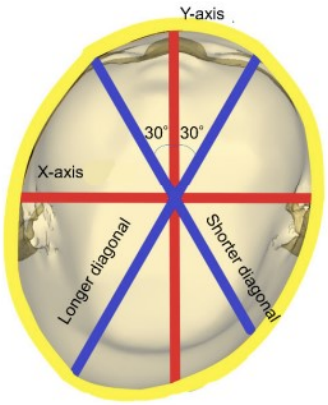

Figure 2.13: Cross-section showing the diagonals used in the diagnosis (retrieved from [40]).

The criterion for assuming that a child has plagiocephaly is CVAI>5%, however there are several degrees of severity, as we can see in the table 2.3.

Table 2.3: Degree of severity taking into account the CVAI (retrieved from [40]).

CVAI	Degree of severity
5% - 6,25%	Smooth
6,25% - 8,75%	Moderate
8,75% - 11%	Severe
>11%	Very Severe

Besides the CVAI, the Plagiocephaly Index (PI) or Cranial Asymmetry Index can also be used, which is obtained through the difference of the diagonals, as can be seen in the figure 2.14.

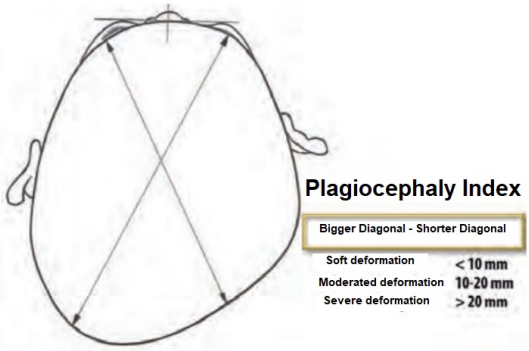

Figure 2.14: Calculation of the Plagiocephaly or Cranial Asymmetry Index (retrieved from [34]).

2.8.4 Brachycephaly

Brachycephaly, known as "short skull", corresponds to about 5,3% of CS and occurs due to early closure of the coronal sutures, bilaterally [32]. Thus, there is a decrease in the anteroposterior diameter and an CI>85%. This cranial dysmorphism may result either from bilateral coronal synostosis or bilateral lambdoid synostosis [17]. The skull is short, with an enlargement of the parietal bones and vertical growth, in an attempt to decompress the brain vertically and towards the temporal region. [17, 18]. Newborns with this CS have less strength in the cervical extensor musculature, which delays the development of motor control of the head and neck [18]. Its diagnosis can also be made by CI, as can be seen in the figure 2.12.

Chapter 3

State of the Art

This chapter reviews the existing literature on the simulation of childbirth.

3.1 Fetal Head Molding

During vaginal delivery, the pressure exerted by the birth canal and surrounding structures causes a molding of the fetal head, which allows for the expulsion of the fetus. In this context, some studies have already been carried out in order to understand which factors influence this phenomenon.

Sorbe and Dahlgren [41] studied fetal head shaping in 319 vaginal deliveries, using a photographic method to record the size and shape of babies' heads immediately after birth as well as 3 days later. To do this, they measured 6 different diameters, however only 3 changed significantly during early neonatal restitution. Furthermore, they calculated a shaping index and compared the results obtained with conventional occipitofrontal circumference. With this, they realised that babies born by primiparous women (women who had their first birth) had significantly higher degrees of head molding than those born by multiparous women (women who had more than one birth). In addition, they also found that oxytocin stimulation during labor, as well as the use of instruments to perform an instrumented vaginal delivery, resulted in increased fetal head molding. Finally, they also analysed the importance of fetal presentation at birth, the duration of labor, the mother's age and the birth weight of the baby with regard to fetal skull molding during labor.

3.2 Computational Modelling and Simulation

With the evolution of technology and the increase in the computational capacity of the machines used in simulation processes it has become possible to build simulation models of dynamic processes and, with these, better understand a given system and its dynamics, as well as develop techniques and tools that allow solving possible problems related to the systems under study [11, 42].

The simulation of natural and physiological processes and phenomena allows, in a simple, rigorous and reliable way, the prediction of events, the investigation of methods and consideration of new methodologies. By simulating, for example, childbirth, it is possible to study, from a biomechanical point of view, the deformations that both the fetus and the pelvic floor suffer during this process. In addition, it can help to study the effectiveness of the instrumentation used in IVD and, if this is not adequate, to understand how its use can be improved.

A key part of ensuring its effectiveness and efficiency is the ability to adapt an existing mesh according to changes that can be made to the geometric CAD (Computer Aided Design) model. Thus, morphing corresponds to a process that allows the adaptation of a pre-existing mesh. The main objective of these techniques is to preserve, in the best possible way, the quality of the element, thus allowing the existence of the largest possible number of geometric changes without the requirement of remeshing due to the inversion of the element [43].

With this, it becomes possible to produce very species-specific geometries suitable for biomechanical modelling, and to do this by adapting a pre-existing model using techniques of morphing [44], on a sampled volumetric representation and, subsequently, apply 3D extensions of image morphing techniques. In this way, the work is performed directly on the mesh, avoiding problems that, generally, volumetric methods present, such as discretization artefacts, high computational cost and difficulty in controlling [45].

Mesh-morphing is a method of modifying the mesh in order to obtain arbitrary shape changes and volume smoothing without changing the mesh topology. Compared to conventional geometry-specific FE modelling techniques, this technique reduces the effort required to generate multiple models of the desired geometry. In the area of FE modelling, this technique is used to adapt the FE model smoothly to other geometries without resorting to the development of new meshes. There are essentially two types of mesh methods: datum-based and surface-matching-based [46].

In fact, mesh transformation allows to modify an existing geometry or a FE mesh by applying a specific distortion. These changes are applied only to the node positions while maintaining the connectivity of the elements. In this way, it is possible to adapt the model to a different geometry without having to create a new model [46].

3.2.1 Biomechanical Simulations of Vaginal Delivery

Biomechanical simulations of vaginal delivery allow us to study the deformations suffered by both the pelvic floor of the parturient woman and the fetal head during delivery. Several studies have been conducted to understand the molding phenomenon of the fetal head during vaginal delivery, as well as the deformations of the maternal pelvis.

To study the phenomenon of fetal head molding during vaginal delivery, Moura *et al.* [1] simulated the second stage of labor, measuring the diameters of the fetal head to assess the degree of molding. They used a FE model of the maternal pelvis and fetal presentation, and replicated the second stage of labor in the occipito-anterior position. By introducing viscoelasticity in the model to evaluate a time-dependent response, they found that a prolonged second stage of labor results in greater molding of the fetal head, and they obtained a percentage molding of 9,1%, resulting from the pressure exerted by the birth canal and surrounding structures. Regarding the pelvic floor muscles, they found a 19,4% reduction in reaction forces and a 2,58% decrease in muscle stretching, indicating that sufficient molding may result in less pelvic floor lesions. This study highlighted the importance of focusing on fetal injuries with non-invasive methods, which may allow anticipating complications during labor [1].

Lapeer and Prager [47] presented a non-linear FE model of the deformation of the complete fetal skull when subjected to cervical pressures during the first stage of labor. Their results are in agreement with those obtained by Sorbe and Dahlgren [41], with regard to the shape of the head after deformation and the degree of deformation. The authors considered that the model created and the simulation performed could be applied in the pediatric field to investigate birth cranial injuries, as well as congenital malformations, such as hydrocephalus.

Bailet *et al.* [48] created a 3D biomechanical model of the fetal head to be associated with a haptic simulator. This model is composed of triangular shell elements with a volume constraint

that guarantees the incompressibility of the fetal head. Furthermore, this model integrates membrane behavior through the use of Constant Strain Triangle (CST) elements, as well as bending behavior, with Discrete Kirchhoff Triangle (DKT) elements. The authors report that their results are in agreement with both the *in vivo* studies carried out by Sorbe and Dahlgren [41], either with the static simulation performed by Lapeer and Prager [47].

Pu *et al.* [49] used a non-linear finite element model of the fetal skull to investigate the deformation of the fetal head with different work forces in the 1st stage of labor, which represents about 90% of the entire duration of labor. The simulation results showed that fetal skull diameter and modified moulding index (MMI) increased when the work force was increased, which highlighted the quantitative relationship between work force and fetal skull molding during labor. In terms of future perspectives, the authors noted that if in the future the degree of fetal skull molding could be directly correlated with head injury, the relationship investigated in this study could be used to predict fetal head injury by measuring the labor force during delivery.

Silva *et al.* [50] used a FE model to represent the effects produced by the passage of the fetal head through the pelvic floor. The model included the pelvic floor muscles attached to the bones as well as the fetal body. The fetal head model included the skin and soft tissues, the skull with sutures and fontanelles, and the brain, and the movements of the fetal head during birth in vertex position were simulated: descent, rotation and extension. Furthermore, two models of the fetal head were compared: a rigid model and a deformable model, the latter including the cranial sutures. Thus, the anatomical indices for the molding of the fetal skull were obtained in order to make a comparison with the clinical data. Furthermore, the influence of the molding of the fetal head on the pelvic floor muscles was studied and it was found that the passage of the deformable head through the birth canal results in a 17,3% reduction in pelvic floor muscle reaction forces compared to those of a rigid head. Regarding the molding of the fetal head, the results obtained are in agreement with clinical experiences.

Jing et *et al.* [51] created an improved model representation of the biomechanics of the levator ani muscle during the second stage of labor and performed a sensitivity analysis to investigate the pathomechanics of levator muscle damage. They created a subject-specific FE model of the human pelvic floor and fetal head based on MRI (Magnetic Resonance Imaging) data. They concluded in this study that the pubovisceral muscle enthesis and the muscle near the perineal body are the areas of greatest strain, putting them at the greatest risk for stretch-related injury. Besides that, they noted the fact that decreasing perineal body tissue stiffness significantly reduced tissue stress and strain, and therefore injury risk, in those regions.

Xuan *et al.* [52] tried to assess the charactheristics of the PFM on the second stage labor to try to investigate the potential pathogenetic mechanism of pelvic floor disorder. So they created a three-dimensional model to explore the influencing factors and characteristics of PFM strength. FE simulations were used in the second stage of labor to analyze the mechanical responses, potential damage, and key parts of postpartum lesions of PFM caused by different fetal DBP sizes. According to the findings, the maximal stress and strain of PFM developed during the first half of the delivery period and at the attachment point of the pubococcygeus to the skeleton. In addition, during the simulation procedure, the pubococcygeus was stretched by around 1,2 times and the levator ani muscle was extended by more than twofold. There was also more stress and strain in the levator ani muscle.

Parente [15] used FEM-based numerical simulations of vaginal delivery to identify the elongations and tensions in the pelvic floor caused by the fetus passage. The FE model utilized in this investigation contained the fetus, the pelvic bones and the PFM linked to the bones. The fetus movements during delivery in cephalic presentation were simulated. The simulations were divided into two groups: those in which the fetus is in an occipito-anterior position and those in which the

fetus is in an occipito-posterior position. In this study, the maximum stretch obtained for both presentations was greater than the maximum stretch obtained in the absence of lesions. So, since injury can be produced by fiber stretch surpassing a maximum allowable value, it may be argued that there is a danger of PFM injury during the second stage of labor. The present numerical simulation demonstrates that the muscles of the pelvic floor are submitted to high deformations during the passage of the fetus head. The levator ani muscle, namely the pubococcygeus muscle, is the muscle that experience the most stretch and tension during a vaginal delivery. These are the muscles that are most vulnerable to a stretch-related injury.

3.2.2 Biomechanical Simulations of IVD using the vacuum-cup

Biomechanical simulations of instrumented vaginal delivery allow the influence of the instruments used to aid delivery to be studied, particularly in terms of the deformations suffered by the maternal pelvis and the fetal head. There are still not many studies in the area of simulation of instrumented vaginal delivery, and those that do exist focus mainly on the impact of childbirth on pelvic muscles.

Estevão [12] carried out a biomechanical analysis of instrumented vaginal delivery (with vacuum-cup) regarding the impact on maternal pelvic floor muscles as well as on the pelvis. Simulations were developed using ABAQUS software, replicating an anterior occipital position of the fetus during the second stage of labor. The results showed that the forces obtained to pull the fetal head were slightly higher than the force exerted by the fetus alone in a non-instrumented vaginal delivery. However, when comparing the results with those of simulations performed in non-instrumented vaginal deliveries, there were no major differences in terms of the deformations suffered by the maternal pelvic floor.

Roriz [13], with the aim of contributing to the clarification of the various mechanisms that interact during an instrumented vaginal delivery, performed numerical simulations based on FEM in order to simulate an instrumented vaginal delivery using the vacuum- cup. With regard to the maximum force, maximum principal stress and maximum logarithmic deformation exerted by the vacuum-cup on the fetal head, the obtained were 12,3 N, 1,812 MPa and 0,216, respectively, for a vertical displacement of the head of 40 mm.

In order to assess the effect of incorrect vacuum-cup position, Lapeer *et al.* [6] performed computer simulations with an FE analysis of the fetal skull bones, fontanelles and vacuum-cup, both for the correct and incorrect positioning of the vacuum-cup, with and without molding of the fetal head. The results obtained show that, with the incorrect positioning of the vacuum-cup, the maximum values for the deformation and rotation of the fetus increase significantly, and, both for the incorrect and correct positioning, when the molding effect is added, these values are worsened.

To study the biomechanical effects of divergent sizes of silicone rubber vacuum extractors during the course of delivery on the fetal head, Huang *et al.* [53] employed a FEM analysis, where they simulated a IVD for different vacuum-cup sizes. First, they created computer models for various vacuum extractor sizes (40 mm, 50 mm, 60 mm, and 70 mm), flat surface, hemispherical ball, and fetal head shapes. The fundamental design for the vacuum extractor model was a hemispherical ball, and the substance used for the vacuum extractor was silicone rubber. Following that, the vacuum extractor displacement was set to 1 mm and the vacuum cap pressure was set to 60 cmHg. This study's major observation markers were the corresponding von Mises stresses on the vacuum extractor and skull caused by the reaction force on the fixed end. The findings demonstrated that larger diameter vacuum extractors cause more response force, stress, and strain on fetal skulls. As a result, the biomechanical analytic implications of this work advise that clinicians should avoid using larger vacuum extractors during operational instrumental delivery so that fetal heads experience less external force, distortion, and problems. It could also serve as a useful reference for obstetricians doing instrumental vaginal delivery using a silicone rubber vacuum extractor.

To sudy the influence of the vacuum-cup material and different pressures on the fetal head during delivery, Chen *et al.* [54] established and performed an FE analytical model to explore the influences of vacuum extractors manufactured from different materials on the fetal head under various extractive pressures. For comparison, the vacuum extractor model was built as a hemispherical form, and the vacuum extractor material was silicone rubber and stainless steel. As criteria for investigation, four different vacuum pressures (500 cmH_2O, 600 cmH_2O, 700 cmH_2O, and 800 cmH_2O) were used. To assess the effects, the reaction force on the fetus head, vacuum extractor von Mises stress, and fetal head skull von Mises stress were measured and studied. The results revealed that different vacuum pressures had subtle divergent influences on the fetal head, and the stainless-steel vacuum extractor induced a greater reaction force (358,040-361,370 N), accompanied by stress (13,547-13,675 MPa), than non-metallic or relatively softer materials. The results provide a reasonable basis for selecting proper vacuum extractor during operational delivery to avoid obstetrical problems, such as scalp scrape, cephalohematoma and even intracerebral hemorrhage.

Chapter 4

Morphing

This chapter presents the methodology used to perform the morphing of the fetal head, as well as the results obtained from the morphing, which were used to perform the simulations.

4.1 Finite Element Method

FEM was developed in the 1950s in the aerospace industry and corresponds to a numerical approach, through which it is possible to solve partial differential equations approximately. This method is widely used in solving engineering problems using computer simulation, especially in stress analysis, heat transfer, fluid flow and electromagnetism. Through these simulations, it becomes possible to predict the behavior of the systems under study, in order to improve performance and design [55].

In this method, the body under study is divided into FE (which are usually just called elements) that are interconnected by nodes, thus forming a mesh of FEs. FEM provides a systematic methodology by which the solution can be determined using a computational software, such as ABAQUS. For linear problems, the solution is determined by solving a system of linear equations, where the number of unknowns is equal to the number of nodes, and in order to obtain a reasonably accurate solution, thousands of nodes are usually required, hence the need to use computers to solve these problems. In fact, as the number of elements (nodes) increases, the accuracy of the solution also increases, however, the computer processing time also increases. In stress analysis displacements correspond to the field variables and, generally, linear analysis is adequate since it is not desirable to have loads that may generate large displacements or originate a non-linear behavior from the material. However, if the objective is to simulate extreme loads, such as collision, a non-linear analysis is necessary [55].

4.2 FE model used

The FE model used, which is represented in figure 4.1, was developed by Moura *et al.* [1] and it was under this that the morphing was carried out for various situations. This model is composed of the skin, sutures and fontanelles (figure 4.1c), skull (figure 4.1b) and brain and has 25459 nodes and 115762 elements. In the figure 4.1 it is presented the model in different perspectives, having the images been taken from ABAQUS.

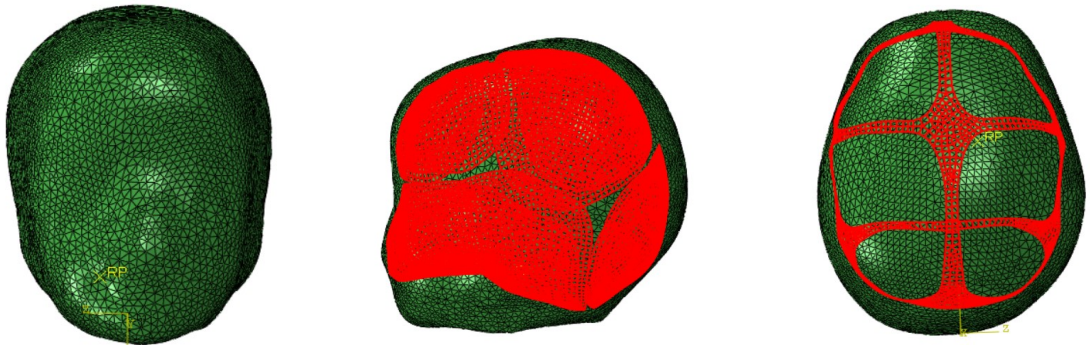

(a) Frontal Plane (b) Sagital Plane (c) Transverse Plane

Figure 4.1: FE model used. In red are (b) bones and (c) sutures.

The skin, skull and brain were modelled with solid tetrahedral elements. Considering that the sutures and fontanelles correspond to the structures that allow the molding of the fetal head, their characteristics should be as close as possible to reality, within the limits of computational modelling. Thus, these structures were modelled with membrane elements in order to obtain a more realistic behavior. The thickness of the sutures and fontanelles was considered constant, with a value of 1,2 mm. These are mainly composed of collagen fibres, extracellular matrix and vascular networks and, thanks to this composition, when a load is applied, the sutures present a viscoelastic behaviour [1].

The properties of each of the structures that make up this FE model were defined according to the parameters shown in the table 4.1, taken from a study conducted by Moura *et. al* [1]. All of them presented an elastic behavior of the isotropic type.

Table 4.1: Properties of the structures that constitute the FE model [1].

Structure	Young's Module (MPa)	Poisson coefficient
Skin	0,3	0,25
Brain	0,0246	0,49
Membranes	3,8	0,45
Bone	250	0,22

4.3 *Morphing*

To perform the morphing of the fetal head, MATLAB was used, adapting Bernardo's code [56] (A), which, in turn, was adapted from the code created by Moura *et al* [1], for each situation under study.

MATLAB is a programming and numerical computing platform that combines an environment adapted for iterative analysis and design processes with a programming language that directly expresses the mathematics of matrices. Among its many applications, those that stood out in the realisation of this project were computational biology and data science [57]. The function that allowed the realisation of morphing was rbfwarp3d. This MATLAB function was aimed at 3D *Point set warping* by the function *thin-plate/rbf* [58]. This corresponds to a radial basis function (RBF), a mathematical function capable of interpolating, providing the exact values at the original points, functions defined only at discrete points (source points). There are several types of radial

functions (inverse quadratic, multiquadratic, among others), however the used one corresponded to a Gaussian RBF [46].

4.3.1 Conditions affecting head size

The methodology chosen to morph the fetal head was to define the DBP and DOF. For that, 4 nodes were selected in order to define these two diameters, as we can see in figure 4.2.

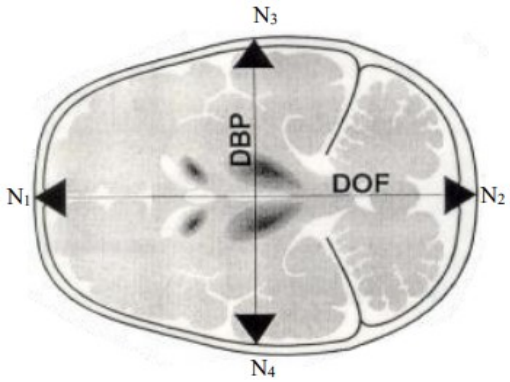

Figure 4.2: Representation of the diameters used and the nodes chosen (adapted from [59]).

Where, N1= 1056, N2=3953, N3=9118, N4=2078 correspond to the mesh nodes used.
The relationship between these diameters and the CP is given by the equation 4.1 [60].

$$CP = (DBP + DOF) * 1,57 \tag{4.1}$$

Based on this relationship, and taking into account the value of the DBP of a fetus considered healthy for each percentile, it was possible to calculate the value of the DOF. Thus, the values found in table 4.2 were used for morphing the various shapes of the fetal head.

Table 4.2: CP, DOF and DBP values used in morphing.

Percentile	CP (cm)	DBP (cm)	DOF (cm)
0,5	32,00	8,600	11,78
2,5	32,60	8,800	11,96
50	34,60	9,400	12,64
97,5	36,60	10,00	13,31

However, there's no data on DBP and DOF, especially when anomalous situations occur at the time of the fetus' birth, as is the case of prematurity and micro and macrocephaly. Thus, in order to be able to carry out the morphing of this type of head, and also because it is especially important in these cases, in which the fetus does not have a "standard head", to understand how the vacuum-cup and the position in which it is placed can induce complications, the weights associated with each of the diameters were calculated, in order to carry out with some degree of confidence in the subsequent calculations.

In order to understand the contribution of each diameter (i.e. its weight and proportions) to the head shape, it was initially considered that both were equal, i.e. if DBP=DOF=D, then:

$$CP = 2D * 1,57 \tag{4.2}$$

Considering the perimeter value for the 0,5th percentile comes:

$$32 = 2D * 1,57 \Leftrightarrow D = 10,19cm \tag{4.3}$$

We know that for a weight of 50%, each diameter measures 10,19 cm. However, from table 4.2 we can see that this is not the value of each of them. So, taking into account the real values of each diameter, we can calculate its weight:

$$p_O = \frac{DOF * 0,5}{D} \Leftrightarrow p_O = \frac{11,78 * 0,5}{10,19} = 0,5780 \tag{4.4}$$

$$p_B = \frac{DBP * 0,5}{D} \Leftrightarrow p_B = \frac{8,600 * 0,5}{10,19} = 0,4220 \tag{4.5}$$

Where p_O and p_B correspond, respectively, to the weight associated with the DOF and DBP. When we want to calculate each of the diameters it is enough, in the equation 4.3 to replace the CP by the value of the perimeter and so we get D. Then, to obtain DOF and DBP we just multiply the value of D by each of the weights, p_O and p_B, as is shown below.

$$CP = D * 1,57 \tag{4.6}$$

$$25,9 = D * 1,57 \Leftrightarrow D = 16,5cm \tag{4.7}$$

$$DBP = 16,5 * 0,422 = 6,96cm \tag{4.8}$$

$$DOF = 16,5 * 0,578 = 9,54cm \tag{4.9}$$

Using this methodology, it was possible to obtain the results presented in table 4.3.

Table 4.3: CP and DBP and DOF values used in morphing of non-standard heads.

Condition	CP (cm)	DBP (cm)	DOF (cm)
Prematurity	25,9	6,96	9,54
Microcephaly	28,0	4,99	6,84
Macrocephaly	38,0	10,2	14,0

It should be noted that microcephaly occurs when the CP is less than 31,9 cm and macrocephaly when it is greater than 36,4 cm. [29]. In this case the values shown in the table were chosen arbitrarily and without any specific reason.

As mentioned before, mesh morphing has as main goal to adapt a new shape to the geometry being studied by updating the nodal positions, preserving and not changing the topology, element and node count. A successful morphing is one in which one is able to update the mesh according to the desired shape modification, preserving as much as possible the quality of the mesh after deformation, i.e., in which the specific shape is preserved and smoothly deforms the surface and volume elements that are within the deformation field, minimizing the distortion of each element [46].

After performing the morphing in MATLAB, input files (.inp) were saved and executed in ABAQUS to verify if the morphing had occurred as intended. For this, it was verified not only

qualitatively the differences between the original mesh and the morphed mesh, but also quantitatively, checking whether the diameters had actually changed.

At first, the DOF and DBP of the original mesh were measured, obtaining values of 10,43 cm and 6,174 cm, respectively. In order to understand whether the values obtained were close to the calculated values, to assess whether the morphing was or was not performed correctly, the relative percentage error associated with each measurement was calculated using the equation 4.10.

$$\varepsilon(\%) = \frac{|Measurement - Calculated|}{Measurement} * 100 \tag{4.10}$$

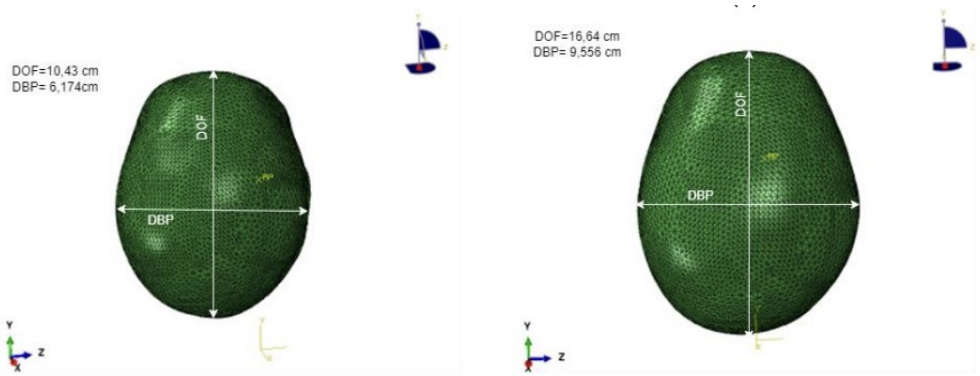

(a) Original mesh (b) Mesh that suffered *morphing*

Figure 4.3: Morphing of the head to a 50th percentile.

In figure 4.3 a comparison is presented between the original mesh and a mesh that underwent morphing for the DOF and DBP relative to a 50th percentile, being these values shown in table 4.2.

In order to verify that the morphing had been correctly performed, both diameters were determined, and a value of 12,64 cm was obtained for DOF and 9,556 cm for DBP. These values are very close to the calculated values, with an associated relative percentage error, obtained using the equation 4.10, of 0,000% for DOF and 1,660% for DBP. Thus, we can consider that, for a 50th percentile, morphing was well achieved.

The same procedure was applied to the remaining study situations, and the results obtained are presented in the table 4.4.

Table 4.4: Values obtained for each diameter and respective relative percentage error.

Situation	DOF (cm)	$\varepsilon(\%)$	DBP (cm)	$\varepsilon(\%)$
P50	12,64	0,000	9,556	1,660
P0,5	11,77	0,08489	8,750	1,744
P2,5	11,95	0,08361	8,951	1,716
P97,5	13,21	0,7513	10,16	1,600
Prematurity	9,500	0,4193	7,099	1,997
Macrocephaly	14,02	0,1429	10,36	1,569
Microcephaly	6,757	1,213	5,120	2,605

As shown in the table 4.4, with the exception of the case of morphing performed for a microcephaly situation, the results obtained are quite similar to the values that were calculated, with the error associated with the DOF being less than 1% and that associated with the DBP being less than 2%. These differences correspond to approximations made in order to try to approximate the new

diameter. Nevertheless, this indicates to us that, for these cases, morphing was well achieved and fulfilled its purpose.

4.3.2 Craniosynostosis

4.3.2.1 Plagiocephaly

To perform morphing for a plagiocephaly situation, it was necessary to define the nodes that outline the major and minor diagonals, as represented in figure 4.4.

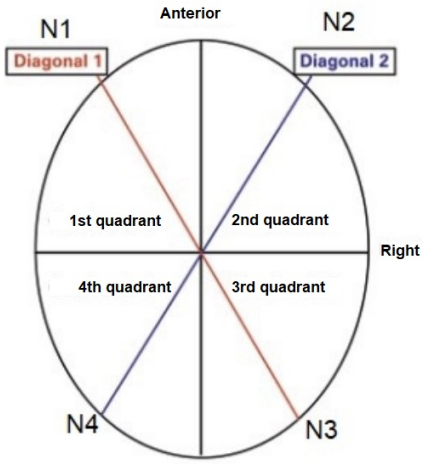

Figure 4.4: Representation of the diameters used and the nodes chosen (adapted from [61]).

Where, N1= 1426, N2=868, N3=5481, N4=68 correspond to the mesh nodes used, which are presented in the figure 4.5.

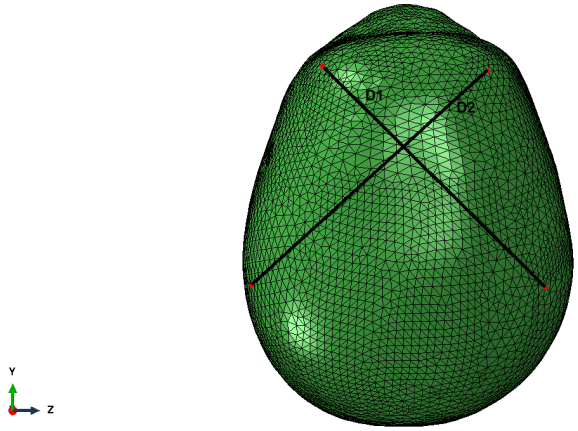

Figure 4.5: Representation of the chosen nodes.

Next, it was necessary to obtain the values of the diagonals of a head considered as normal. Thus, based on these nodes, were obtained, in the original mesh [56], the values of the diagonals, being these 101,161 mm and 103,416 mm for diagonals 1 (D1) and 2 (D2), respectively. For these values we have an associated PI of 2,255 mm.

Based on the data illustrated in figure 2.14, for the morphing of a head with moderate plagiocephaly, a PI of 12,255 mm was considered. Based on this same image, and knowing that, generally, in this type of craniosynostosis there is a decrease in volume in quadrant 3, represented in figure 4.4, a decrease of 5 mm in D1 and an increase of 5 mm in D2 were considered, giving a D1 of 96,161 mm and a D2 of 108,416 mm (thus obtaining a PI of 12,255 mm).

As in this craniosynostosis only the occipital part is affected, nodes were fixed in the frontal part of the head (nodes 8215, 10296 and 10631), as shown in figure 4.6, so that these do not suffer morphing.

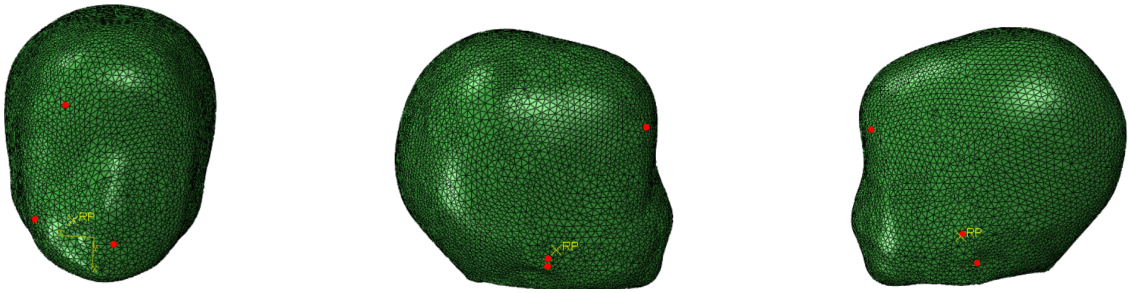

Figure 4.6: Representation of the nodes that have been fixed.

The morphing was divided into 2 phases. Firstly, diagonal 2 (right diagonal) was changed, morphing was performed and the resulting nodes were saved. In a second step, the nodes that resulted from the 1st morphing were used (figure 4.7), and morphing was performed on these, in which diagonal 1 (left diagonal) was changed (figure 4.4). The commands used to define the values of the diagonals were the same used by Bernardo [56], however, a modification was made so that there were only changes in the occipital part, following the commands shown in figure 4.8.

```
%% READ NODE FILES
%%%% HEAD NODES
fileID = fopen('head_nodes_1stmorph.inp','rt');
headerChars = fgetl(fileID);
data_n = fscanf(fileID,'%f,%f,%f,%f',[4 Inf]).';
```

Figure 4.7: Import of the nodes of the first morphing.

```
%%%% Right Oblique diameter %%%%
dim1 = ODR1;
dim2 = ODR2;

p1 = find(id_lmk == dim1);
p2 = find(id_lmk == dim2);

a1 = data_n(dim1,2:4);
a2 = data_n(dim2,2:4);

old_d_x = abs(a1(1)-a2(1));
old_d_y = abs(a1(2)-a2(2));
old_d_z = abs(a1(3)-a2(3));
old_d_min = min([old_d_x old_d_y old_d_z]);
old_d = pdist2(a1,a2);
new_d = 96.161;


if old_d_min == old_d_x
    THETA = atan((a1(3)-a2(3))/(a1(2)-a2(2)));

    if old_d > new_d
        THET1 = ((old_d-new_d)*sin(THETA))/2;
        THET2 = ((old_d-new_d)*cos(THETA))/2;
        %na1(3) = a1(3)+THET1;
        na2(3) = a2(3)+2*THET1;
        %na1(2) = a1(2)+THET2;
        na2(2) = a2(2)+2*THET2;
    else
        THET1 = ((new_d-old_d)*sin(THETA))/2;
        THET2 = ((new_d-old_d)*cos(THETA))/2;
        na1(3) = a1(3)-THET1;
        na2(3) = a2(3)+THET1;
        na1(2) = a1(2)-THET2;
        na2(2) = a2(2)+THET2;
    end
```

Figure 4.8: Changes that have been made to diagonal 1.

4.3.2.2 Scaphocephaly

As shown in figure 2.12, in scaphocephaly, the CI changes, taking into account the degree of severity. Thus, for the morphing of this craniosynostosis, with a moderate degree, a CI of 66,9% was considered, with the DOF=112 mm and the DBP=75 mm.

In this case, morphing was carried out in one step and allowed the DOF and DBP to be changed, however, the commands used, shown in figure 4.9, have allowed for the alteration of the head as a whole, and not just the occipital part.

4.3.2.3 Brachycephaly

Similarly to what happened in the case of plagiocephaly, in order to perform the morphing of a fetal head with brachycephaly we started by fixing some frontal nodes, as represented in figure 4.6. Based on the CI values shown in figure 2.12, an CI value of 83% was considered, with the DOF=90,4 mm and the DBP=75 mm, using the nodes represented in figure 4.2 to set these diameters.

For the brachycephaly case, morphing was carried out in a single phase, following the reasoning of the algorithm shown in figure 4.8, applied to each of the diameters to be changed (in this case, DOF and DBP). Moreover, for this condition, similarly to plagiocephaly, changes were only performed in the occipital part of the head.

```
%% DEFINE NEW HEAD DIAMETERS
%% Occipital frontal diameter %%%%
dim1 = OFD1;
dim2 = OFD2;

p1 = find(id_lmk == dim1);
p2 = find(id_lmk == dim2);

a1 = data_n(dim1,2:4);
a2 = data_n(dim2,2:4);

old_d_x = abs(a1(1)-a2(1));
old_d_y = abs(a1(2)-a2(2));
old_d_z = abs(a1(3)-a2(3));
old_d_min = min([old_d_x old_d_y old_d_z]);
old_d = pdist2(a1,a2);
new_d = 112;

if old_d_min == old_d_x
    THETA = atan((a1(3)-a2(3))/(a1(2)-a2(2)));

    if old_d > new_d
        THET1 = ((old_d-new_d)*sin(THETA))/2;
        THET2 = ((old_d-new_d)*cos(THETA))/2;
        na1(3) = a1(3)+THET1;
        na2(3) = a2(3)-THET1;
        na1(2) = a1(2)+THET2;
        na2(2) = a2(2)-THET2;

    else
        THET1 = ((new_d-old_d)*sin(THETA))/2;
        THET2 = ((new_d-old_d)*cos(THETA))/2;
        na1(3) = a1(3)-THET1;
        na2(3) = a2(3)+THET1;
        na1(2) = a1(2)-THET2;
        na2(2) = a2(2)+THET2;
    end
```

Figure 4.9: Changes that have been made to the DOF.

4.3.2.4 Mesh analysis

After performing morphing in MATLAB, the input files (.inp) were saved and subsequently executed in ABAQUS in order to verify if the morphing had occurred as intended. To this end, the differences between the original mesh and the morphed mesh, but also quantitatively, checking whether the diameters had actually changed.

Qualitatively, the meshes for the 3 craniosynostoses have suffered the intended deformations, as can be seen in figure 4.10.

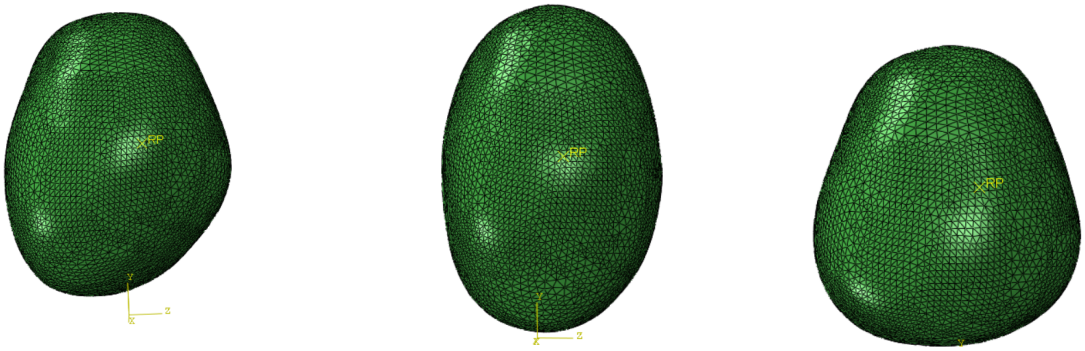

(a) Plagiocephaly (b) Scaphocephaly (c) Brachycephaly

Figure 4.10: FE mesh obtained after performing morphing for each of the craniosynostoses under study.

In the case of plagiocephaly, quantitatively, the values of diagonals 1 and 2 (figure 4.4) were measured in ABAQUS , having obtained, respectively, the values of 96,161 mm and 108,420 mm. It can be seen that the values obtained are identical to the assigned values, with an associated relative percentage error of around 0,001%, which proves that the morphing was carried out as intended.

For the scaphycephaly, the DOF and DBP values were measured in ABAQUS, and 112,0 mm and 75,00 mm were obtained respectively. The values obtained correspond to the assigned values, with an associated relative percentage error of 0,003%, which demonstrates that the morphing was successful.

Finally, for brachycephaly, similarly to what happened with scaphycephaly, the values of DOF and DBP were measured, obtaining 95,228 mm and 86,518 mm, respectively. Of the three situations under study, this was the one that resulted in the most dissonant values, with a relative percentage error of approximately 5,340% for the DOF and 15,360% for the DBP. Although qualitatively the mesh presents the desired aspect, the morphing has a higher relative error, which indicates the need to optimise the algorithm used for situations in which the deformations are more pronounced and involve more than one quadrant of the head.

In order to understand in what way the morphing performed on the mesh changed its quality, for each one of the situations, using ABAQUS, a mesh quality analysis was performed, since a poor quality mesh can reduce the accuracy of the results or even generate totally unpredictable results [62].

Each FE is designed to function correctly within certain ranges of element distortion before it degenerates, i.e. before two or more nodes fall on the same coordinate. The amount of distortion allowed before degenerating depends mainly on the type of element and the numerical procedure used in the formulation of the element [62]. There are different types of measurements that can be carried out to quantify the distortion of the elements and thus avoid their degeneration. So, at first, for each of the situations, the elements with a weak shape (warnings) and those that were degenerated (errors) were determined, as shown in figure 4.11.

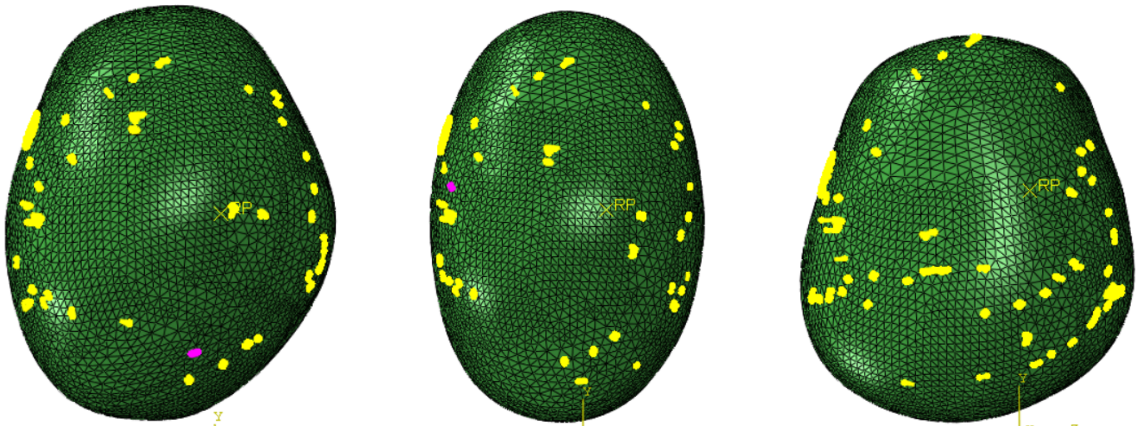

(a) Plagiocephaly (b) Scaphocephaly (c) Brachycephaly

Figure 4.11: Quantification of the distortion of elements, where yellow is for warnings and pink is for errors.

For plagiocephaly, 165 warnings (0,142534%) and 1 error (0,00086%) were identified. In the scaphocephaly mesh, 1 error and 163 warnings (0,140806%) were also identified. Finally, for brachycephaly no error was identified, however 213 warnings (0,183998%) were highlighted.

The second test performed consisted of the "Face Corner Angle" test, which allows verifying how much the element departs from its ideal shape (obliquity), by calculating the face corner angles of the element. Besides this, the proportion test was also performed. This refers to the relationship between the largest and smallest characteristic dimension of an element. High aspect ratio values are associated with a greater inaccuracy of the FE representation and may have a detrimental effect on the convergence of the FE solution [62].The criteria selected to perform these tests are shown in table 4.5.

Table 4.5: Limit Selection Criteria (retrieved from [63]).

Selection Criteria	Quadrilateral	Triangular
Corner angle of smallest face	10	5
Corner angle of the largest face	160	170
Aspect ratio	10	10

The results obtained for the triangular elements are shown in table 4.6 and for quadrangular elements in table 4.7.

Table 4.6: Results obtained for triangular elements.

Criteria	Plagiocephaly	Scaphocephaly	Brachycephaly
Minimum angle < 5	23 (0,0216691%)	23 (0,0216691%)	27 (0,0254376%)
Minimum average angle	37,68	37,46	35,96
Worst minimum angle	0,0201	0,0197	0,0225
Maximum angle > 170	2 (0,00188427%)	2 (0,00188427%)	2 (0,00188427%)
Maximum average angle	89,48	89,80	91,78
Worst maximum angle	171,15	170,27	172,31
Aspect ratio >10	13 (0,0122477%)	13 (0,0122477%)	13 (0,0122477%)
Average aspect ratio	1,74	1,75	1,82

Table 4.7: Results obtained for quadrangular elements.

Criteria	Plagiocephaly	Scaphocephaly	Brachycephaly
Minimum angle < 10	1 (0,010395%)	1 (0,010395%)	1 (0,010395%)
Minimum average angle	78,35	78,03	76,69
Worst minimum angle	0,14	0,16	0,14
Maximum angle > 160	0	0	0
Maximum average angle	102,43	102,75	103,99
Worst maximum angle	148,07	150,20	154,21
Aspect ratio >10	3 (0,031185%)	3 (0,031185%)	3 (0,031185%)
Average aspect ratio	1,81	1,83	1,84

It is important to bear in mind that each mesh has 106142 triangular elements and 9620 quadrangular elements. Taking that into account, and by analysing the tables 4.6 and 4.7, it is noticeable that the number of elements that deviate from their ideal shape is not high, i.e., there is a not very substantial number of elements that deviate from their ideal shape, which will affect the quality of the mesh, but not in such a way as to make its use unfeasible.

Then, the changes suffered by the sutures and fontanelles in each morphing were evaluated, as represented in figure 4.12.

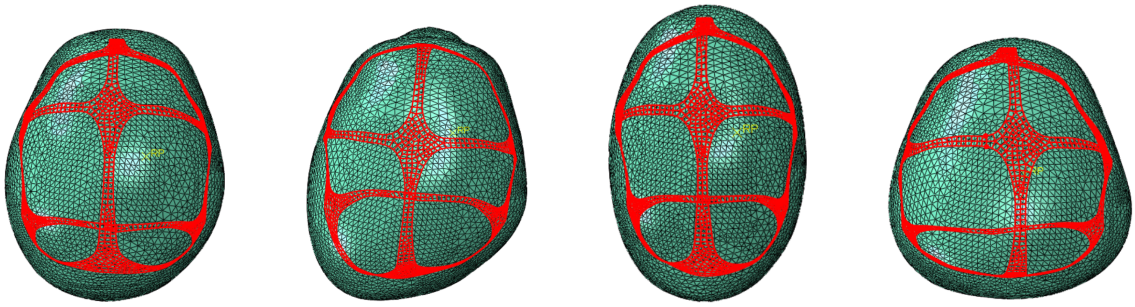

(a) Normal (b) Plagiocephaly (c) Scaphocephaly (d) Brachycephaly

Figure 4.12: Modification of the sutures and fontanelles (in red) in each situation.

As previously mentioned, the craniosynostoses under study are due to the early closure of one or more sutures (figure 2.11). Thus, in order to quantify the modifications suffered by each suture, associated to each of the situations, their width was measured and compared to the original width (measured in the normal mesh, at the same two points).

In plagiocephaly, there is early closure of the coronal suture, in this case the right coronal suture, and its width was then measured in the normal mesh and in the plagiocephalic mesh. The normal mesh had a width of 4,759 mm and the morphing mesh 4,666 mm. The width decreased, as intended, but the reduction was not as accentuated as it should have been (there was a reduction of only 1,960%).

In a situation of scaphocephaly, the sagittal suture closes early. Its width in the normal mesh had a value of 3,734 mm and in the mesh that underwent morphing it had a value of 3,590 mm, with an associated decrease of 3,850% in width.

In brachycephaly there is early closure of the coronal sutures bilaterally. The right coronal suture had a width of 4,759 mm in the normal mesh and 5,273 mm in the modified mesh, and, contrary to expectations, its width increased by 10,790%. The left coronal suture had a width of 5,276 mm in the normal mesh and 5,833 mm in the modified mesh, increasing its width by 10,560%. Thus, in this case, there was no early closure of the sutures, therefore, although the head presented the intended shape, this did not happen, taking into account the mechanisms that, in the fetal head, lead to this asymmetry.

Finally, the size of the fontanelles was evaluated for each situation, in order to understand the modifications suffered by them, for each situation. The same points were always considered, removing the measurements as shown in figures 4.13 and 4.14.

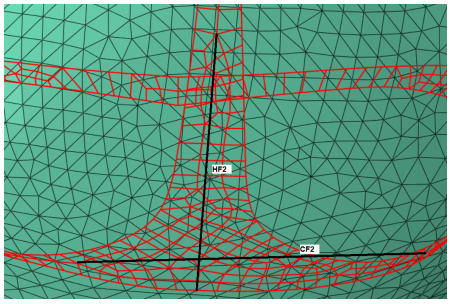

Figure 4.13: Measurement of the posterior fontanelle size.

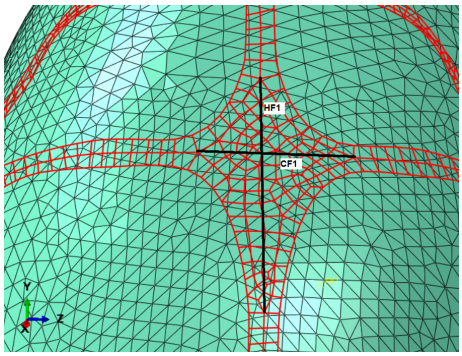

Figure 4.14: Measurement of the anterior fontanelle size.

Where HF1 and HF2 correspond, respectively, to the height of the anterior and posterior fontanelles and CF1 and CF2 to their lengths. The results obtained are shown in table 4.8.

Table 4.8: Results obtained for fontanelle size.

Measurement (mm)	Normal	Plagiocephaly	Scaphocephaly	Brachycephaly
Anterior fontanelle height	29,784	29,451	29,326	31,650
Anterior fontanelle length	18,560	18,325	18,128	18,378
Posterior fontanelle height	36,690	34,345	44,625	—
Posterior fontanelle length	35,233	34,099	30,584	—

As far as concerns the anterior fontanelle, with the exception of brachycephaly, its size was slightly reduced (in the order of 1,500%). For the posterior fontanelle, in brachycephaly, as can be seen in figure 4.12d, this has disappeared, hence in table 4.8 no values are presented. In plagiocephaly, its size decreased, and in scaphocephaly, its length also decreased, while its height increased by around 21,600%.

Effectively, these results corroborate the premise previously presented that, in the brachycephaly situation, although qualitatively the mesh presents the desired aspect, the morphing was not performed in a way to mimic the mechanisms that generate this asymmetry. In fact, this is one of the most complex craniosynostosis, as it affects more than one quadrant of the head, which, by itself, may originate more complications when performing morphing.

Chapter 5

Biomechanical Simulations

This chapter presents the biomechanical simulations performed, as well as their results.

5.1 FE models used

As in the majority of biomechanical studies presented in the chapter 3, FEM was used in compputational simulations in order to study the biomechanical changes suffered by the pelvic floor of the parturient during vaginal delivery. Thus, in order to simulate this process as reliably as possible, geometric models that represent the maternal pelvic anatomy, such as the bones and muscles of the pelvic floor, as well the model of the fetal head were used.

5.1.1 Fetal Head FE model

Following the procedure presented in chapter 4, but considering a new model that defines the fetal head as a rigid body, morphing was performed again for plagiocephaly and scaphycephaly.

The mesh chosen to continue the project, namely in terms of simulations, was the mesh that mimics a situation of scaphocephaly, for presenting a good quality and for being the craniosynostosis with the highest incidence. So all the simulations and results presented are related to a head that has scaphocephaly.

5.1.2 Pelvic Floor FE Model

The pelvic floor is composed of a group of muscles and fascias of the female urogenital region. During pregnancy, together with the abdominal muscles, it is these that support the weight of the fetus, which generates an overload during the various months, making normal childbirth violent for these muscless [64].

The pelvic floor model used, shown in figure 5.1, was the one developed by Moura *et al.* in the study [1], having been modelled with a modified form of the transversely isotropic incompressible hyperelastic model proposed by Martins *et al.* [65] and the constitutive parameters were obtained from Parente *et al.* [66].

The model is composed of the illiococcygeus muscle, represented in orange in the figure 5.1, and by the pubovisceral structure, represented in red, these having been modelled with hexahedral elements with hybrid formulation (C3D8H). The surface represented in grey (rigid quadrilateral shell elements) in figure 5.1 delimits the anterior region, imposing the limits that are anatomically

ensured by the birth canal, replacing the anterior part of the pelvic bones. This surface allows the translation of the fetal head in the anteroposterior direction, ensuring a surface of soft contact between the fetal head and the replaced pelvic bones, improving the convergence of the simulations [1].

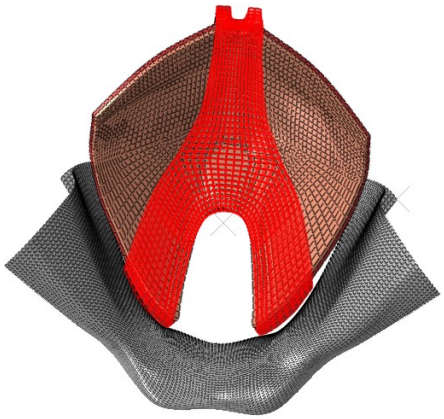

Figure 5.1: FE model of the maternal pelvis.

5.1.3 FE Vacuum-Cup Model

The FE model of the silicon vacuum-cup, represented in figure 5.2, was developed by Estevão [12], being the *Kiwi Omnicup Vacuum Device* developed by *Clinic Innovations*, because it is the most widely used instrument in Portugal and because it is available at FEUP.

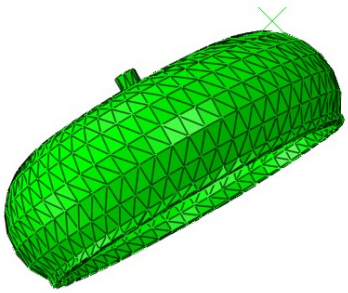

Figure 5.2: FE Vacuum-cup model.

The measures used in the model were those used by Roriz [13], so a diameter of 50 mm and a height of 20 mm were defined. The mesh is composed of 7146 linear tetrahedral elements of type C3D4 (general purpose tetrahedral element with onde integration point) and 13553 nodes. Although hexahedral elements are more accurate in computer simulations, the vacuum-cup is not a structure where the results will be read, hence the choice of tetrahedral elements [12].

5.2 Positioning of the vacuum-cup

As mentioned in chapter 2, the correct positioning of the vacuum-cup is fundamental to ensure that the IVD occurs without any major concerns. Currently, there's a defined flexion point on the fetal head, 3 cm from the posterior fontanelle, as shown in figure 5.3 [21].

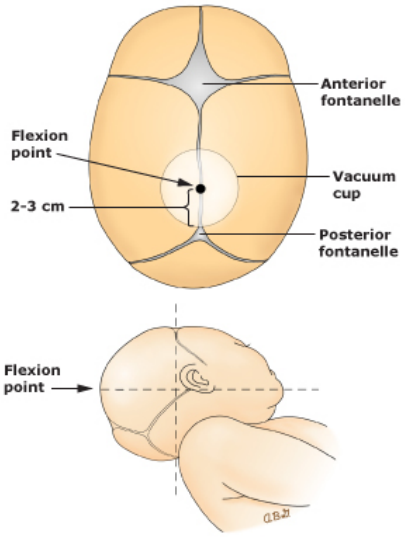

Figure 5.3: Flexion Point in relation to fetal skull landmarks (retrieved from [67]).

Taking this in consideration, using FEMAP the vacuum-cup was placed, as represented in figure 5.4.

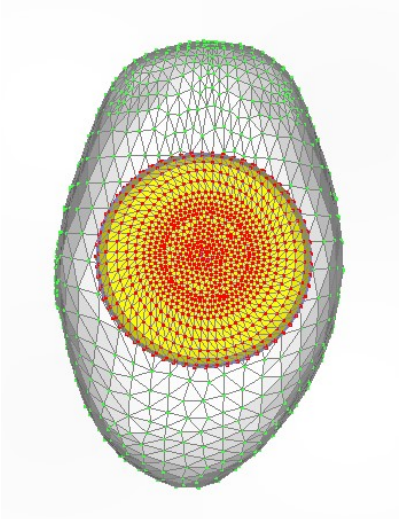

Figure 5.4: Position of the vacuum-cup.

5.3 Simulations

The simulations performed were adapted from those carried out by Moura *et al.* [1]. These were performed in ABAQUS to mimic the second stage of labor, in a vertex presentation and occipito-anterior position, where the aim was to assess the consequences of delivering a fetus with scaphocephaly, both with and without a vacuum-cup, on the pelvic floor of the mother. All the movements of the fetal head are imposed by the reference node, which controls its translation and rotation during the different steps of the simulation, which begins with complete cervical dilation and ends with the passage of the head.

The standard ABAQUS contact algorithm was used to impose the kinematic contact conditions, and contact constraints were established between the fetal head skin and the pelvic floor muscles, and between the fetal head skin and the pelvic bones. To create these conditions, a surface interaction with the Augmented Lagrange method was used. Regarding the boundary conditions, the nodes corresponding to the ends of the pelvic floor muscles, the pubic bone and the pelvic fascia connecting to the pelvic bone were fixed.

With regard to the duration of labor, in nulliparous women (who have never had a birth) the average duration of the second stage is highly variable [68]. The normal duration of a birth is between 30 min and 180 min [4]. If the duration is shorter or longer, we are dealing with a hasty or prolonged birth, respectively. There were performed simulations, where the birth was simulated with a duration of 100 min and, also, simulations with the birth having the duration of 150 min.

5.3.1 Simulation without the vacuum-cup

The first simulations performed were without the vacuum-cup, for a delivery time of 100 min and 150 min. As previously mentioned, the passage of the rigid head through the birth canal was simulated using ABAQUS and a step-by-step approach. The first step of the simulation consisted in aligning the head with the birth canal, and the subsequent steps consisted in lowering the head and adapting the maternal pelvis to this passage.

In this simulations, the movements of the fetus were fully controlled, and for that to happen, a reference node in the middle of the fetal head was assigned to an element with rigid properties. Thus, the flexion and extension of the fetal head, corresponding to the cardinal movements, can be performed by controlling the displacements and rotations of this node, causing the vertical descent of the fetus.

In a first moment the stretch suffered by the maternal pelvis along the normalised trajectory in the lowest portion of the pelvic floor was evaluated (figure 5.5), taking into account the vertical displacement suffered by the foetal head.

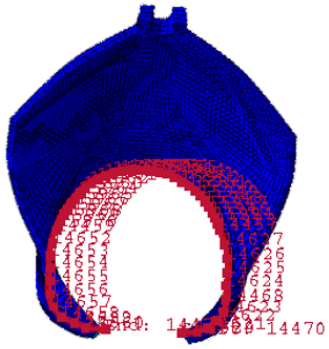

Figure 5.5: Normalised trajectory in the lowest portion of the pelvic floor.

According to Lien *et al.*, a stretch above 1,5 may indicate that the muscles have suffered considerable damage [69].

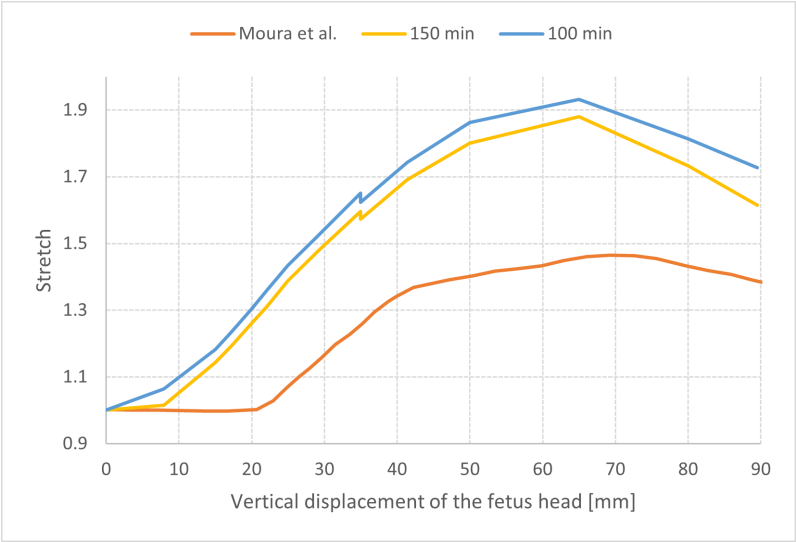

Figure 5.6: Stretch calculated along the normalised trajectory at the lowest portion of the pelvic floor.

As can be seen in figure 5.6, that presents a comparison between the stretch obtained in this study for both delivery times, and that obtained in the study developed by Moura *et al.* [1].In this study, a maximum stretch of 1,93 and 1,88 was obtained, for the respective delivery times, corresponding to a vertical displacement of 65 mm, which indicates that, in this case, the muscles of the maternal pelvis most probably suffered considerable injuries. Furthermore, the results obtained indicate that, although not with a significant difference, that stretch decreases with increasing duration of labor. Comparing these results with the results obtained in the study by Moura *et al.*, there was an increase of about 31% in the stretch. It's important to note that in the studied performed by Moura *et al.*, it was used a deformable head that didn't suffered morphing, so a normal head instead of a head with scaphocephaly.

Next, the maximum principal Cauchy stresses were analysed for two key moments of the simulation: its end and the maximum stretch moment.

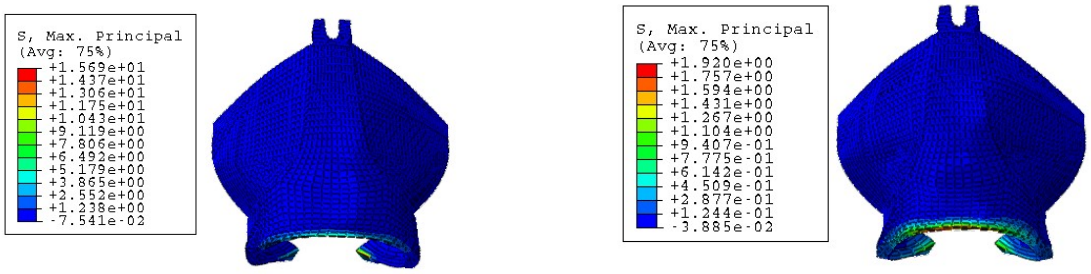

(a) Maximum stretch instant. (b) End of the simulation.

Figure 5.7: Distribution of maximal Cauchy principal stresses (MPa) in pelvic floor muscles for a delivery duration of 100 minutes.

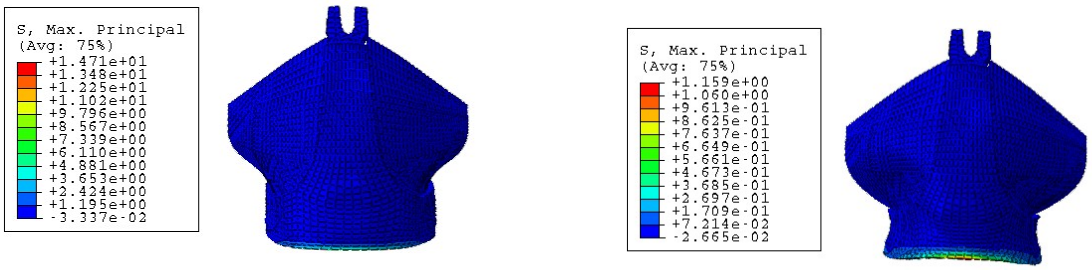

(a) Maximum stretch instant. (b) End of the simulation.

Figure 5.8: Distribution of maximal Cauchy principal stresses (MPa) in pelvic floor muscles for a delivery duration of 150 minutes.

As it can be seen in figure 5.7, for a delivery duration of 100 minutes in the first we have a maximum stress of about 15,69 MPa, while in the other a maximum stress of 1,920 MPa. For a delivery duration of 150 minutes, for the moment of maximum stretch we have a maximum stress of 14,71 MPa and for the end of the simulation a maximum stress of 1,159 MPa, as can be seen in figure 5.8.

Comparing in terms of the duration of labor, the results show a reduction of about 6,25% for the moment of maximum stretch and 39,63% at the end of the simulation, for an increase of 50 minutes in the duration of labor.

Finally, the reaction forces were analysed in relation to the vertical displacement, and their magnitude is represented in figure 5.9.

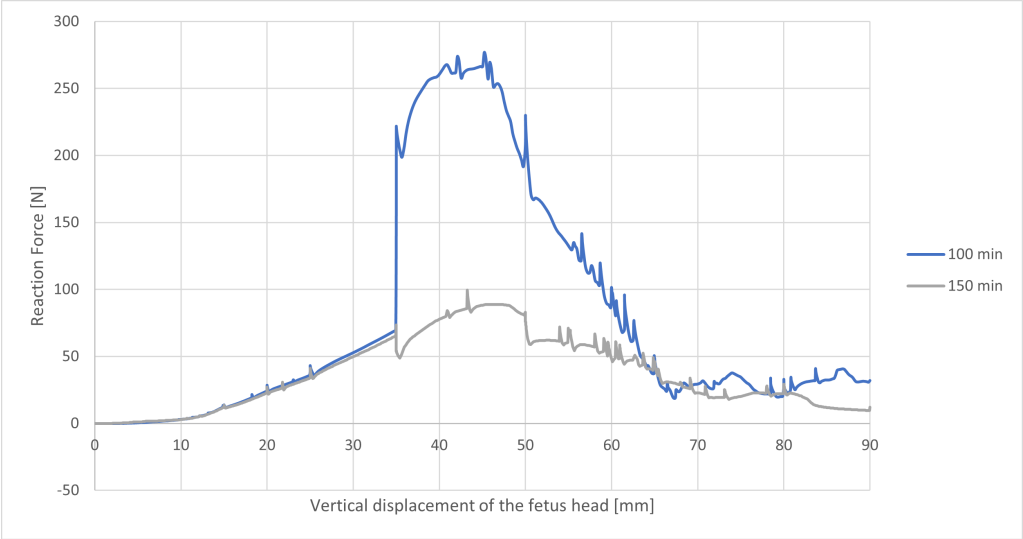

Figure 5.9: Reaction forces in relation to vertical displacement.

As it's seen in figure 5.9, the reaction forces magnitude decreased around 3 times when the delivery time increased 50 minutes. This was not expected, because, with increasing length of labor, the muscles are under stress for longer and therefore the reaction forces should not decrease. Compared to the study performed by Moura *et al.* [1], that also used a delivery time of 100 minutes, the forces obtained were about 10x higher, however the model of the pelvis used was not the same, and furthermore, in this study the fetal head used was a rigid body, while in the other it was a mouldable head. Thus, given all these results, it is most likely that the simulation for the 100 min suffered some kind of error.

5.3.2 Simulation with the vacuum-cup

After performing the simulation without the vacuum-cup, this instrument was introduced in the simulation in order to study its influence.

In a second phase, after fulfilling the prerequisites for placing the vacuum-cup on the fetal head, its descent was no longer controlled by the reference node on the head, but by a reference node on the vacuum-cup. This reference node was placed in the centre of the vacuum-cup, where, in the real model, the tension wire is connected. To keep the fetal head and the vacuum-cup connected during the simulations, a binding constraint was used between the two surfaces (tie constraint), so that once connected to each other, one cannot separate from the other until the end of the simulation, i.e. after the fetal head has completely passed through the pelvic floor.

In this simulation only the control was passed to the vacuum–cup, maintaining the downward trajectory.

We started by assessing the stretch suffered by the maternal pelvis along the normalised trajectory in the lowest portion of the pelvic floor (figure 5.5), taking into account the vertical displacement suffered by the fetal head, and the comparison between a 100 min and a 150 min delivery time is represented in figure 5.10.

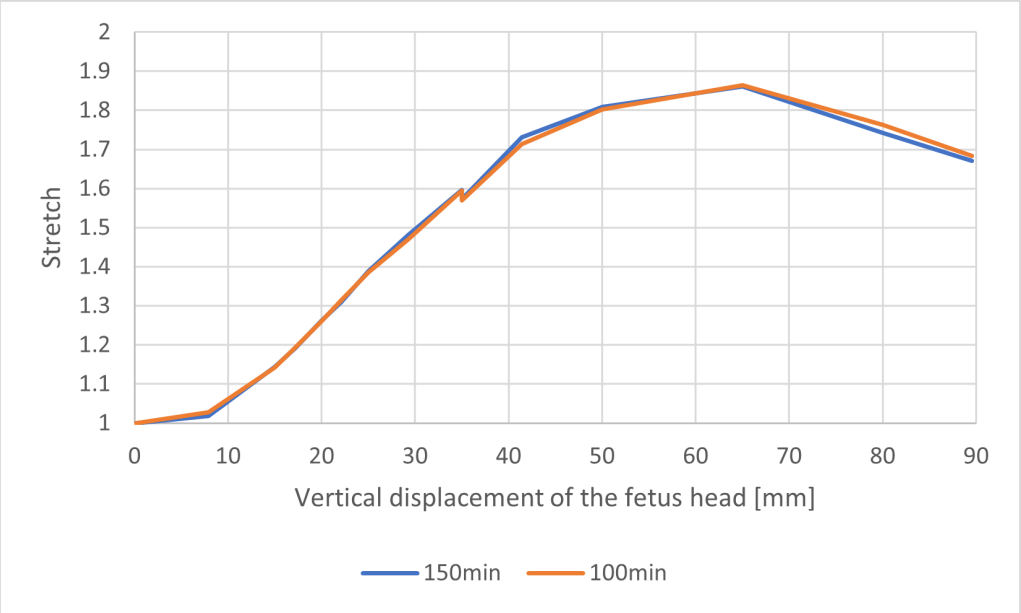

Figure 5.10: Stretch calculated along the normalised trajectory in the lowest portion of the pelvic floor.

As it can be seen in the previous figure, the results obtained show that the stretch with the vacuum-cup is not influenced by the delivery time. In fact, as the geometry remains, the stretch is supposed to be similar, despite the time difference.

The representation of the interaction between the 3 models is presented in figure 5.10, for the moment of maximum stretch.

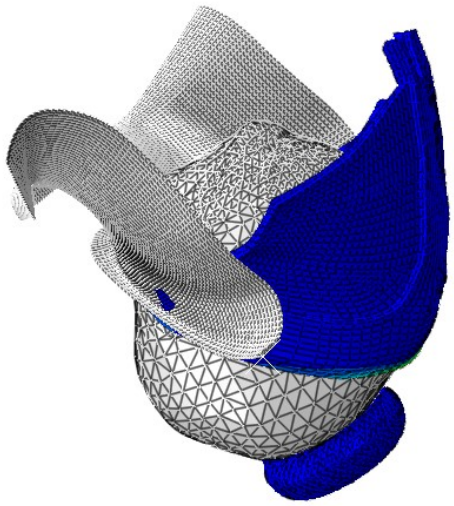

Figure 5.11: Simulation at the moment of maximum stretch.

Adopting the same procedure that was performed in the simulation without vacuum-cup, the maximum principal Cauchy stresses for the maximum stretch moment and end of the simulation

were analysed, these being presented in figures 5.12 and 5.13.

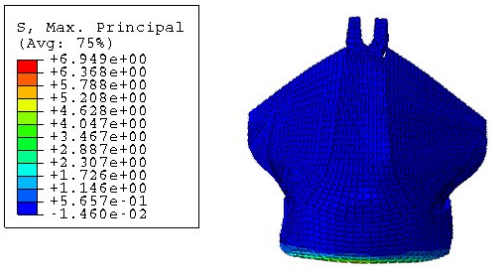

(a) Maximum stretch instant.

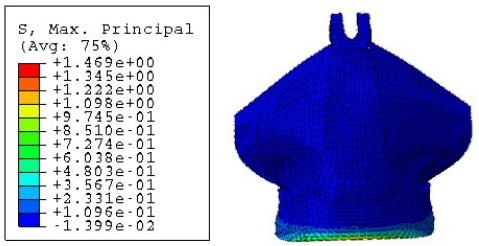

(b) End of the simulation.

Figure 5.12: Distribution of maximum principal Cauchy tensions (MPa) in the pelvic floor muscles for a delivery duration of 100 minutes.

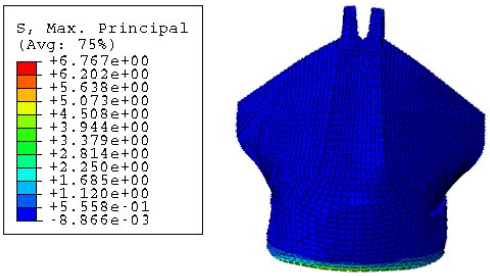

(a) Maximum stretch instant.

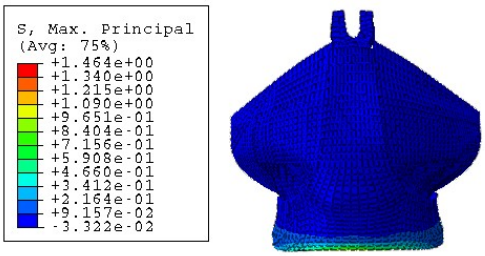

(b) End of the simulation.

Figure 5.13: Distribution of maximum principal Cauchy tensions (MPa) in the pelvic floor muscles for a delivery duration of 150 minutes.

For a delivery duration of 100 minutes, for the moment of maximum stretch we have a maximum stress of about 6,949 MPa, while in the end of the simulation a maximum stress of 1,469 MPa. For a delivery duration of 150 minutes, for the moment of maximum stretch we have a maximum stress of 6,767 MPa and for the end of the simulation a maximum stress of 1,464 MPa. In this case, there was an increase of about 2,61% in the maximum stress for the moment of maximum stretch, and a decrease of about 0,34% for the end of the simulation, with the increase of 50 minutes on the duration of the delivery. The results are not very consistent, which may indicate that there was some simulation error.

Finally, the reaction forces were analysed in relation to the vertical displacement, and their magnitude is represented in figure 5.14.

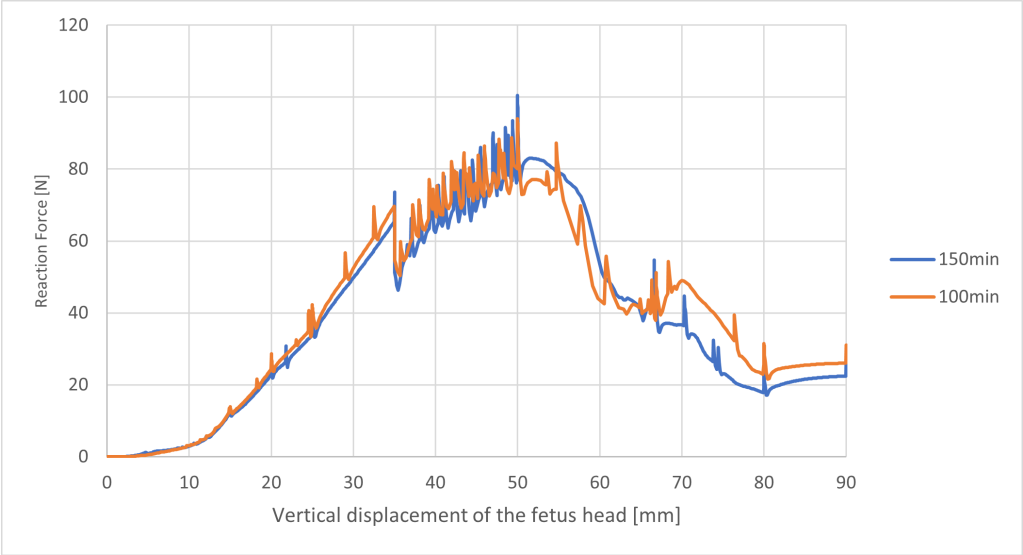

Figure 5.14: Reaction forces in relation to vertical displacement.

In terms of reaction forces, the results obtained don't show a considerable influence of delivery time when the vacuum-cup is used.

5.3.3 Influence of the vacuum-cup

The main aim of this study was to study the influence of the vacuum-cup on childbirth. There were performed simulations were the varying factors were: presence of the vacuum-cup and delivery time. For each delivery time it will be analysed the influence of the vacuum-cup on the pelvic floor muscles.

5.3.3.1 Delivery time: 100 minutes

Firstly, it was studied the influence of the vacuum-cup in the stretch.

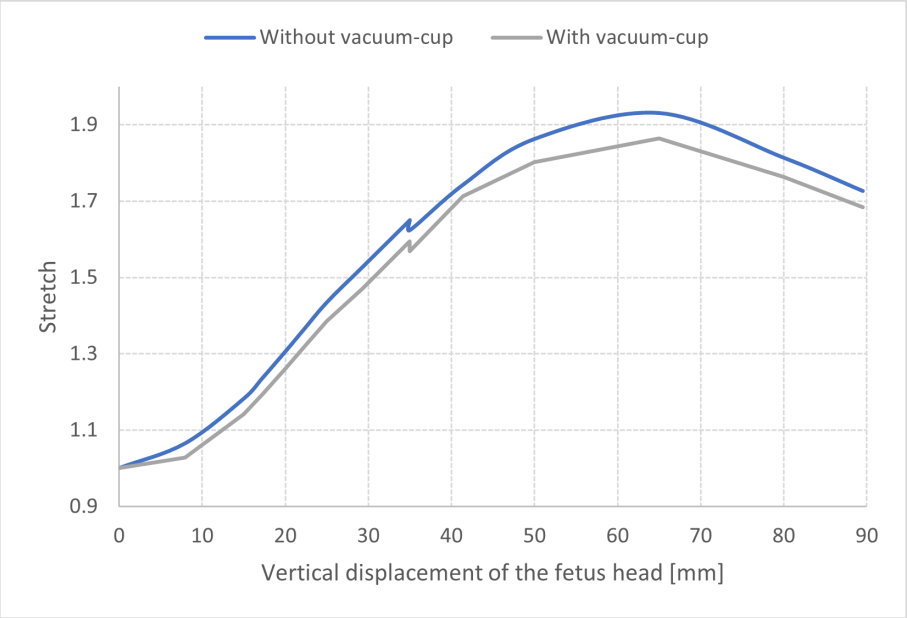

Figure 5.15: Stretch calculated along the normalised trajectory in the lowest portion of the pelvic floor.

As can be seen in figure 5.15, that presents a comparison between the stretch obtained with and without the vacuum-cup in the study developed, a maximum stretch of 1,93 and 1,86 was obtained, without and with the vacuum-cup, respectively, corresponding to a vertical displacement of 65 mm, which indicates that, in this case, the muscles of the maternal pelvis most probably suffered considerable injuries. The curve obtained with the vacuum-cup has the same shape as the curve obtained without the vacuum-cup, however, contrary to what was expected, the stretch value decreased with the use of the vacuum-cup. This may be the result of the fact that, when adapting the simulation to the use of the vacuum-cup, the head acquired a more correct positioning, since, at the moment of maximum stretch, a rotation along the z-axis was introduced to optimise the position of the vacuum-up in relation to the pelvic floor.

The maximum Cauchy stresses previously presented are presented in table 5.1, to perform a comparison for a delivery duration of 100 minutes regarding the influence of the vacuum-cup.

Table 5.1: Maximum Cauchy stress for a delivery duration of 100 minutes.

Timing of the simulation	Without the vacuum-cup	With the vacuum-cup
Maximum stretch moment	15,69 MPa	6,949 MPa
End of the simulation	1,920 MPa	1,469 MPa

Comparing the maximum stress values, a decrease of about 56% was obtained for the maximum stretch situation and of about 23% at the end of the simulation with the use of the vacuum-cup, which is not in accordance with what was expected.

Finally, the reaction forces were analysed in relation to the vertical displacement, and their magnitude is represented in figure 5.16.

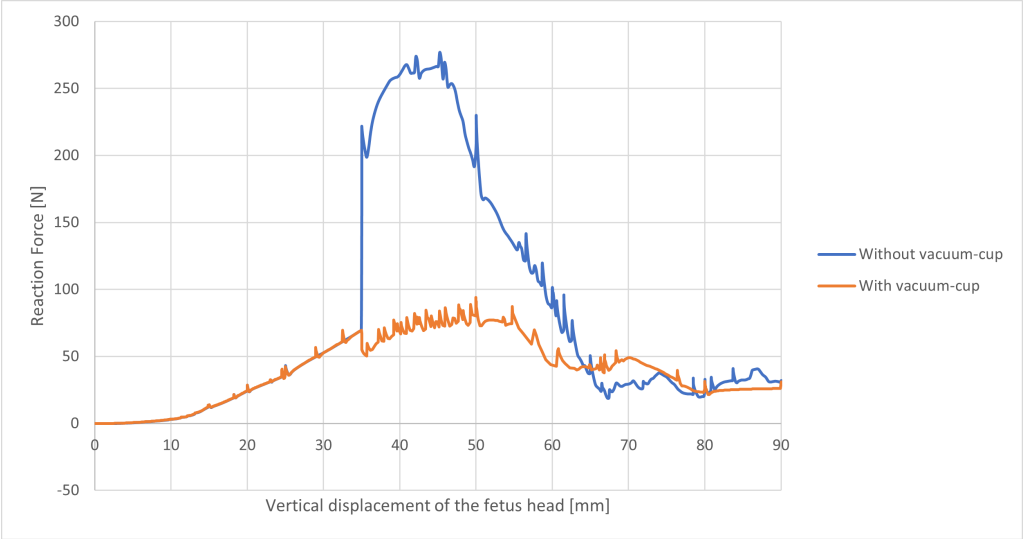

Figure 5.16: Reaction forces in relation to vertical displacement.

Analysing the figure 5.16, it is noticeable that, until the 35mm of vertical displacement of the fetal head, the reaction forces were the same, which is as expected since, in this displacement interval, there was no influence of the vacuum-cup and, therefore, the conditions were the same for both simulations. However, for a displacement between 35 mm and 65 mm, the reaction forces decreased about 61% for the simulation with vacuum-cup, which is not in accordance with what was expected, since in this interval there was only the influence of the vacuum-cup after 50 mm. These results are closer to the results obtained in the study performed by Moura *et al.* [1]. Compared with the simulation without the vacuum-cup, there was still an decrease of about 77% in the magnitude of the reaction forces when the vacuum-cup is added. From 65 mm of displacement onwards, there is the influence of the vacuum-cup, and between 65 mm and 80 mm there was an increase of about 40% in the reaction forces, which is in accordance with what was expected. Moreover, it is important to mention that in this interval a slight rotation of the head was introduced in order to better position the suction cup. Finally, between 80 mm and 90 mm there was a slight decrease in the reaction forces, however, at this stage of the simulation the head is practically all outside the pelvic floor. Taking into account the rotation introduced previously, the results obtained in this range can be justified with a more adequate positioning of the head.

5.3.3.2 Delivery time: 150 minutes

The maximum Cauchy stresses previously presented are presented in table 5.2, to perform a comparison for a delivery duration of 150 minutes regarding the influence of the vacuum-cup.

Table 5.2: Maximum Cauchy stress for a delivery duration of 150 minutes.

Timing of the simulation	Without the vacuum-cup	With the vacuum-cup
Maximum stretch moment	14,71 MPa	6,767 MPa
End of the simulation	1,159 MPa	1,464 MPa

Comparing the maximum stress values, a decrease of about 54% was obtained for the maximum stretch situation and of about 26% at the end of the simulation with the use of the vacuum-cup, which is not in accordance with what was expected.

For a delivery time of 150 minutes, the influence of the vacuum-cup on the stretch is presented in figure 5.17.

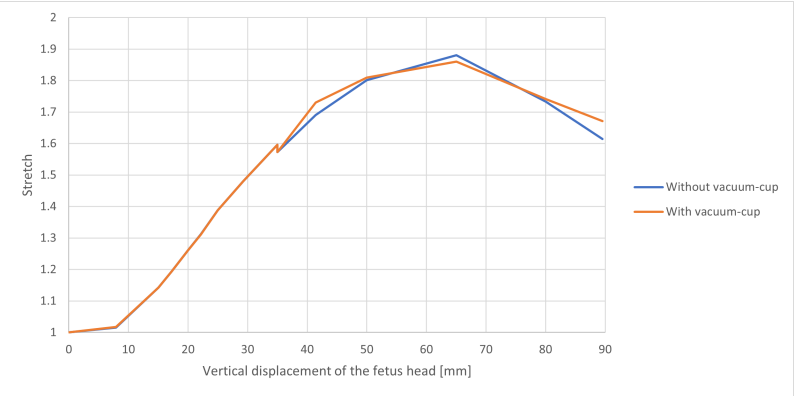

Figure 5.17: Stretch calculated along the normalised trajectory in the lowest portion of the pelvic floor.

The results show that, for a delivery time of 150 minutes, the use of the vacuum-cup doesn't have a big influence in terms of stretch. However, the stretch is the same with and without the vacuum-cup untill a vertical displacement of 35 mm, but it should be similar untill a vertical displacement of 50 mm, since the vacuum-cup was only introduced in this point.

Finally, the reaction forces were analysed in relation to the vertical displacement, and their magnitude is represented in figure 5.16.

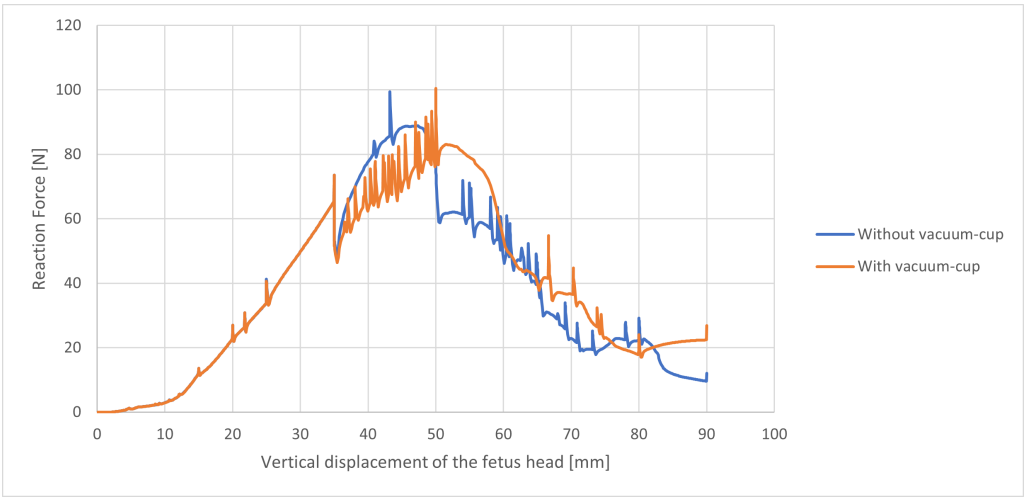

Figure 5.18: Reaction forces in relation to vertical displacement.

Analysing the figure 5.18, it is noticeable that, until the 35 mm of vertical displacement of the fetal head, the reaction forces were the same, which is as expected since, in this displacement interval, there was no influence of the vacuum-cup and, therefore, the conditions were the same for both simulations. However, between 35 mm and 50 mm displacement the reaction forces decreased for the simulation with vacuum-cup, which is not in accordance with what was expected,

since in this interval there was not yet the influence of the vacuum-cup. From 50 mm of displacement onwards, we start to have the influence of the vacuum-cup, and it's seen slight variations in the reaction forces, however not with a linear behavior (in some intervals they increase and in other they decrease).

Chapter 6

Additive Manufacturing

In order to visually demonstrate to obstetricians the differences between an asymmetric and a symmetric (and standard) head, craniosynostosis models were printed using additive manufacturing.

6.1 Additive Manufacturing

Additive Manufacturing (AM) is a digital technology used to produce physical objects from a 3D CAD file. This technology is governed by the principle of adding material, layer by layer [70].

There are several AM techniques, using different materials and operating modes, as can be seen in figure 6.1.

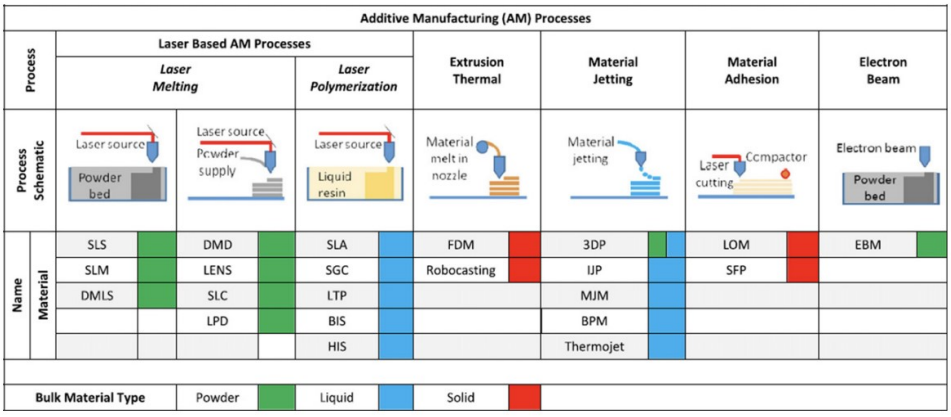

Figure 6.1: Material categories for AM technologies (retrieved from [71]).

AM can deliver parts with very intricate and complex geometries, with minimal need for post-processing, which are built from tailored materials, associated with almost zero material waste, and is applicable to a wide variety of materials, including plastics and metals. In this way, AM is a tool that offers greater "design freedom" and allows designers and engineers to create unique products that can be manufactured in small volumes and economically [71].

This technology has several benefits, including [70]:

- No need to use tools, which significantly reduces production time and costs.
- The production of small batches becomes feasible and economical.

- Possibility of quickly changing the design.
- Allows the product to be optimised in terms of function.
- Reduction of material waste.
- Possibility of producing customised parts, which becomes extremely important in the medical area, namely in the production of prostheses and implants adapted to each patient.

6.2 Printer and materials used

There are several AM techniques and numerous pieces of equipment available. Thus, an appropriate selection of one that meets the required application criteria is necessary [72].

The techniques chosen were FDM (*Fused Deposition Modelling*) and LCD (Liquid Crystal DisplaY). The materials were PLA (Polylactic Acid) and Water washable resin (esun), respectively, and the printers PrusaSlicer and phrozen, given the objective of the printing and because they were available at FEUP.

6.2.1 FDM

6.2.1.1 PLA

PLA is a biodegradable thermoplastic, of natural origin and from renewable sources, which has good printing characteristics, namely [73]:

- Be easy to print and can be used in any printer, whether open or closed, with or without a heated table;
- Has good adherence to the printing table;
- It has a low shrinkage;
- It has a high superficial hardness;
- Has a high visual quality in printing;
- Originates shiny pieces;
- Confers an excellent adhesion between layers.

6.2.1.2 FDM

FDM is an additive manufacturing process in which a thin filament of a thermoplastic is fed into a machine where a printhead heats it to its melting temperature and extrudes it to a thickness of typically 0,25 mm, as shown in the figure 6.2 [74, 75].

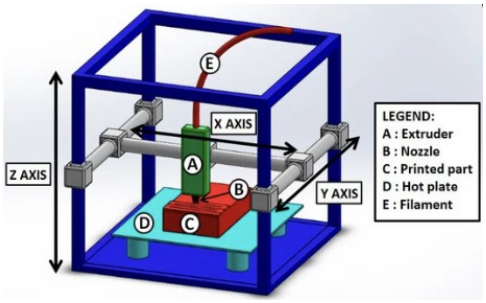

Figure 6.2: Schematic representation of a typical FDM configuration (retrieved from [76]).

The main advantages of this process are that there is no need for chemical post-processing or the use of curing resins. In addition, machines and materials are less expensive, resulting in a more economical process. The disadvantages are that the resolution in the z-axis is low compared to other additive manufacturing processes, so if a smooth surface is required, a finishing process is necessary. Also, it is a slow process, sometimes taking days to build large and complex parts [75].

In this manufacturing technique, the parts are made layer by layer. When the marks of these layers become visible on the printed part, you get the perception of a staircase, and the thickness of the layer is one of the parameters that most influences the staircase effect. Very thin layers reduce the ladder effect, resulting in a smooth and continuous surface, while thicker layers show greater evidence of this effect, resulting in a rougher surface. Figure 6.3 shows the layered section of a CAD model where the ladder effect is visible [77].

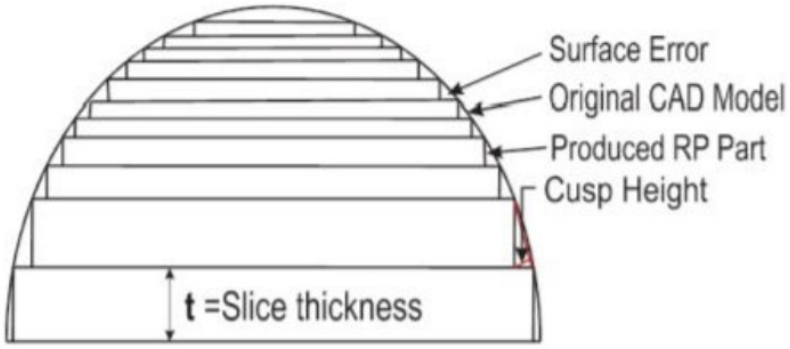

Figure 6.3: Staircase effect (retrieved from [77]).

6.2.1.3 3D Models

The print settings selected were as follows:

- Print settings: 0,20 mm QUALITY @MK4
- Filament: Prusament PLA
- Printer: Original Prusa MK4 0.4 nozzle
- Supports: everywhere

- Infill: 15%
- Scale: 25%

In terms of the parameters concerning the layers, the infill and the supports, these were setted as presented in figure 6.4.

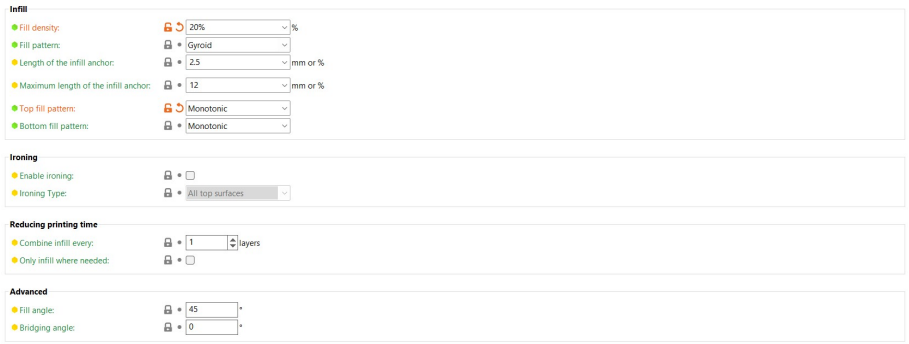

(a) Infill Parameters

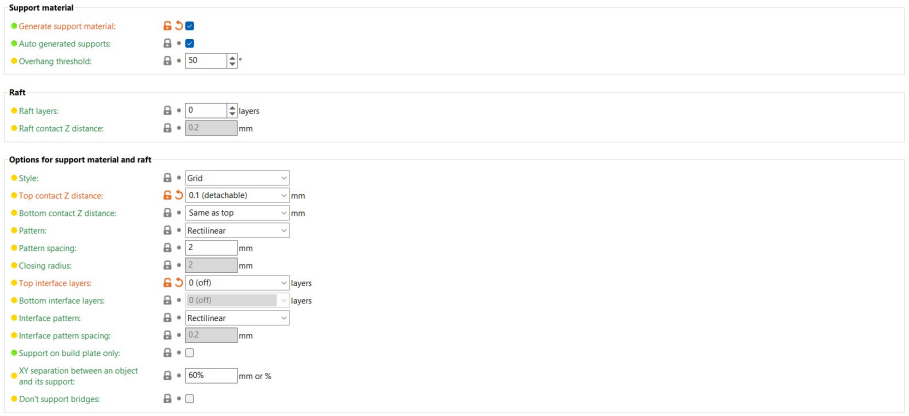

(b) Supports Parameters

(c) Layers and Perimeters Parameters

Figure 6.4: Parameters for FDM.

The import model of each head was made in .OBJ format and each was positioned in the way that seemed most suitable for printing, as shown in the figure 6.5, and also added the supports that seemed appropriate.

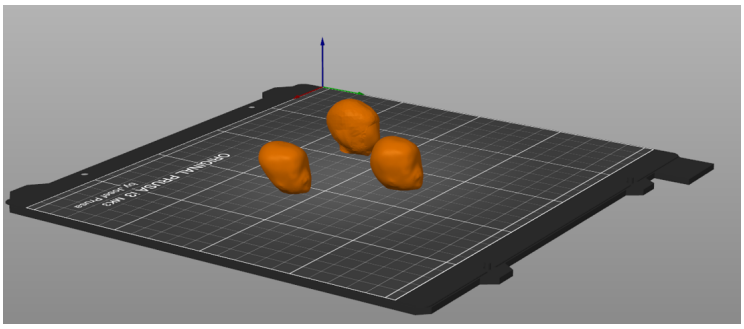

Figure 6.5: Models for FDM.

6.2.2 LCD

6.2.2.1 Water washable resin (esun)

The material used was the water washable resin provided ny esun. This resin has an excellent molding precision eith high resolution, and the surface of the printed object is smooth, being the details visible. Besides that, it has balanced mechanical properties, like strength, toughness and rigidity. It has low viscosity, which results in a high release rate, being easy to print. This resin can be washed with water,taking the need for alcohol cleaning, shortening the post-processing time.So, water washable resin can improve the printing efficiency and be cost-effective [78].

6.2.2.2 LCD

LCD is a laser based AM process using resin where a UV light coming from an array of LEDs shining through an LCD flashes complete layers at the resin tank. The liquid resin is contained within a vat, or tank, cured against a build platform, which slowly rises out of the tank as the part is formed, layer by layer. This technique is a cost-effective resin manufacturing technique to get big and detailed functional parts, focusing on mass manufacture and large component 3D printing for resin materials [79].

6.2.2.3 3D models

The import model of each head was made in .OBJ format and each was positioned in the way that seemed most suitable for printing, as shown in the figure 6.6, and also added the supports that seemed appropriate. The heads were printed simultaneously and it's size was reduced.

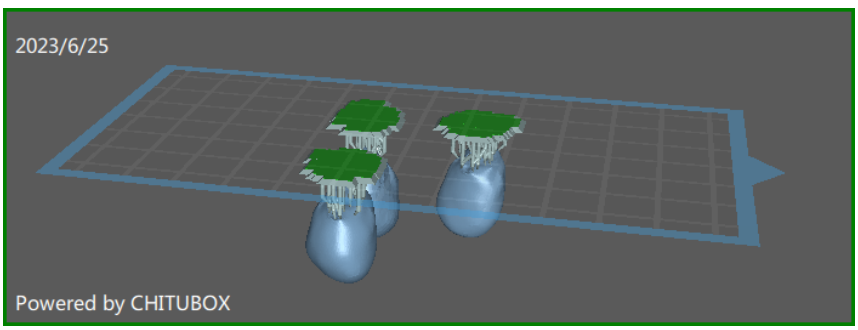

Figure 6.6: Models for LCD.

Chapter 7

Conclusion

The simulation of biological processes has emerged in the area of Medicine, as a complement of case studies and the development of therapies and improvement of conventional procedures. Childbirth comprises a complex and unpredictable mechanism, and the methodologies used in this process are applicable to the general population, but in more unusual cases they may have severe consequences. The use of the vacuum-cup in assisted childbirth allows minimizing the trauma to the fetus at birth, however, if placed in the wrong position, it may injure and cause damage to the newborn, as well as the parturient. In fact, the ideal position of the vacuum-cup is defined for the great majority of heads, however, for heads with more unusual shapes, the adoption of the same position may not be the most correct practice. Therefore, it is important to study the effects of using the vacuum-cup on different head shapes, considering the defined flexion point. To this end, biomechanical simulation is a key tool.

In order to be able to carry out this study, it is necessary to to develop different meshes, corresponding to different head models. In this study, firstly it was performed the morphing of different types of symmetrical fetal heads, taking into account different percentiles and birth conditions, such as prematurity and macrocephaly. Next, it was also performed the morphing of asymmetrical heads, namely heads with plagiocephaly, scaphycephaly and brachycephaly. To this end, MATLAB was used to perform the morphing itself, taking into account data from the literature and extrapolated data. ABAQUS allowed to understand the state of the mesh and to analyse the internal structures of the head. In general, the developed algorithm was able to performed the desired morphing and to change the mesh as idealized, qualitatively, with the meshes presenting the intended aspect, and quantitatively with relatively reduced relative percentage errors, especially in the cases of plagiocephaly and scaphycephaly. However, for the case of brachycephaly, the obtained values of morphing deviated considerably from the attributed values. Regarding the evaluation of the mesh quality, taking into account the number of elements that each one had, it was not obtained a very high number of errors (degenerate elements) and warnings (weakly shaped elements). In order to verify how far the elements were from their ideal shape, the "Face Corner Angle" test was performed, and taking into account the number of elements of each mesh, the results obtained show that there are not many elements that depart from their ideal shape, which, despite affecting the quality of the mesh, does not make its use unfeasible.

In order to understand the modifications that some of the internal structures of the head suffered with morphing, the modifications suffered by the sutures and fontanelles in each situation were evaluated. In plagiocephaly and scaphycephaly, the size of the sutures suffered a slightly

accentuated decrease, while in brachycephaly, the size of the sutures involved increased considerably, which is not in accordance with what was expected, as in craniosynostosis there is early closure of the sutures and their size should have decreased. As far as fontanelle size is concerned, in plagiocephaly and scaphycephaly the anterior fontanelle decreased in size, while in brachycephaly it increased in size. The posterior fontanelle in brachycephaly disappeared and in the other two situations it underwent more modifications in terms of size when compared to the anterior fontanelle. These results, together with those previously presented, demonstrate that, for a situation involving the modification of more than one quadrant of the head, as is the case of brachycephaly, there are more complications in performing morphing and that, therefore, the algorithm could be optimized for these cases.

The morphing carried out allowed us to study the influence of the vacuum-cup on the fetal head, in order to understand its impact both in situations where the head presents symmetry and normal sizes, and in situations where it does not. The next step then consisted in simulating the birth, and, for this, the scaphycephalic head was chosen to continue the study. FEM was used in computer simulations in order to study the biomechanical changes suffered by the pelvic floor of the parturient during vaginal delivery, first without the use of the vacuum-cup, and then using this instrument.

The first simulations performed were without the use of the vacuum-cup, varying only the duration of the birth, between 100 and 150 minutes. In these simulations, even with the increase of the birth duration in 50 minutes, the stretch remained similar. The maximum Cauchy stress, on the other hand, decreased with the increase in the duration of labor for the moment of maximum stretch and at the end of the simulation. Finally, the reaction forces decreased with the increase in the duration of labor, which is not as expected since, with the increase of this time, the muscles are under stress for longer and, therefore, the reaction forces should not decrease.

Then, the previous simulations were repeated with the introduction of the vacuum-cup. In this case, both the stretch and the reaction forces remained constant despite the increase in the duration of labor. The maximum Cauchy stress showed the same behaviour as in the simulation without vacuum-cup.

Finally, for each duration of labor, the influence of the vacuum-cup was studied. Both for a duration of 100 minutes and for a duration of 150 minutes, the stretch remained similar with and without the vacuum-cup, and the maximum Cauchy stress decreased with the addition of the vacuum-cup both for the moment of maximum stretch and at the end of the simulation. The reaction forces, on the other hand, remained constant for a duration of 150 minutes, however, for a labor of 100 minutes they decreased with the introduction of the vacuum-cup, which is another evidence that, most likely, the simulation without vacuum-cup for 100 minutes suffered some kind of error.

The last step of the project consisted in the additive manufacturing of the craniosynostosis heads, using FDM technology, PLA as the material and the PrusaSlicer printer for this purpose. The different printing parameters were adapted to the needs of the project.

In order to complement this study, future morphing could be performed for the missing craniosynostosis (trigonocephaly). In terms of simulation, it would be interesting to repeat the biomechanical simulation with and without vacuum-cup, however for other head shapes, and moreover for a deformable head. Furthermore, it would be interesting to perform the simulation for different vacuum-cup positions and formats, also including an extra force to better simulate the action of the vacuum-cup, for different delivery times (for instance, a prolonged delivery time) and introducing a fetal head rotation.

Appendix A

Appendix

A.0.1 Abstract submitted to the National Congress of Biomechanics (CNB)

10º CONGRESSO NACIONAL DE BIOMECÂNICA
Ana Amaro, Luis Roseiro et al. (Eds)
Figueira da Foz, Portugal, 5-6 de maio, 2023

AVALIAÇÃO DO IMPACTO DA COLOCAÇÃO DA VENTOSA EM POSIÇÕES DISTINTAS DURANTE O PARTO VAGINAL INSTRUMENTADO

Erica Ferreira [1] e Dulce Oliveira [2]

[1] Departamento de Engenharia Física, FEUP, Portugal, up202103363@fe.up.pt
[1] INEGI, Porto, Portugal, doliveira@inegi.up.pt

PALAVRAS-CHAVE: Biomecânica, Craniossinostoses, Método dos Elementos Finitos, Modelação Computacional, *Morphing*.

RESUMO: *O parto envolve extensas alterações fisiológicas na parturiente para permitir a passagem do feto através do canal de parto. Em certos casos, pode existir a necessidade de realizar um parto instrumentado, sendo a ventosa o instrumento de eleição. Apesar de ser uma prática amplamente utilizada, ainda existem incertezas quanto ao local ideal para colocar a ventosa, especialmente quando estamos perante cabeças assimétricas. Neste trabalho, foi realizado o morphing de diversas morfologias de cabeças fetais recorrendo ao MATLAB para este efeito, e ao ABAQUS para avaliação da qualidade do morphing. Os resultados obtidos serão, posteriormente, utilizados para a realização de simulações do parto instrumentado com ventosa, de forma a avaliar as implicações das diferentes posições possíveis para a ventosa na cabeça do feto e nos músculos maternos.*

1 INTRODUÇÃO

O parto é um processo natural e fisiológico bastante complexo, que depende da morfologia e configuração da pelve materna, bem como da contratilidade uterina e do tamanho fetal [1,2]. Quando o curso do parto não é favorável, este pode ser realizado com o auxílio de instrumentos, como é o caso da ventosa, que permite minimizar os traumas no feto [3]. A colocação correta da ventosa é crucial para garantir o sucesso do processo de extração com ventosa. Atualmente, há um ponto de flexão na cabeça fetal estabelecido como o ideal para a colocação da ventosa, mas isso pode não ser apropriado para cabeças fetais com morfologias incomuns. As implicações do ponto de colocação da ventosa na cabeça do feto e nos músculos maternos precisam de ser avaliadas.

Os modelos computacionais são ferramentas valiosas que permitem analisar os mecanismos do parto de uma forma não invasiva.

2 METODOLOGIA

Neste trabalho foi realizado o *morphing* de diversas morfologias de cabeças fetais, com o intuito de, num trabalho futuro, se simular as deformações que estas cabeças sofrem por intermédio da ventosa. Para tal, recorreu-se ao MATLAB, tendo-se adaptado um algoritmo que permitisse realizar o *morphing* destas cabeças desenvolvido por Bernardo [4], tendo por base o modelo de elementos finitos (EF) desenvolvido por Moura et al. [5], que se encontra apresentado na figura 1.

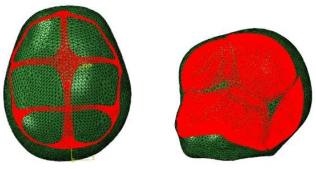

(a) (b)

Fig. 1 Modelo de EF utilizado. A vermelho encontram-se em (a) as suturas e em (b) os ossos.

Além de se ter realizado o *morphing* para diversos percentis, incluindo prematuridade e macrocefalia, este foi, também, realizado para situações que introduziam assimetrias na cabeça (craniossinostoses), nomeadamente em casos de plagiocefalia, escafocefalia e braquicefalia. Para garantir o sucesso do *morphing*, recorreu-se ao *software* ABAQUS.

A metodologia escolhida para realizar o *morphing* da cabeça fetal para diferentes percentis passou pela definição dos diâmetros biparietal (DBP) e occipitofrontal (DOF) e pelo estabelecimento da sua relação com o perímetro cefálico. Para o caso das craniossinostoses, foi necessário estabelecer outros diâmetros e relações entre os mesmos, de forma a provocar a deformação desejada.

3 RESULTADOS E DISCUSSÃO

Após a realização do *morphing* no MATLAB, foram guardados ficheiros de *input* que foram depois executados no ABAQUS.

Para os casos em que se variou apenas o tamanho da cabeça, mantendo a forma, de forma a aferir se o *morphing* foi ou não realizado corretamente, foi calculado o erro relativo percentual associado a cada medição, encontrando-se registados na tabela 1.

Tab. 1 - Valores obtidos para cada diâmetro e respetivo erro relativo percentual.

Caso	DOF (cm)	ϵ (%)	DBP (cm)	ϵ (%)
Macrocefalia	14,02	0,1429	10,36	1,569
Prematuridade	9,500	0,4193	7,099	1,997

Para os casos de craniossinostoses, foi avaliada qualitativamente a malha, observando se esta apresentava a forma pretendida, e quantitativamente, verificando se os diâmetros selecionados se tinham modificado conforme o pretendido. Na figura 2 encontra-se, a título de exemplo, o resultado do *morphing* realizado para um caso de plagiocefalia.

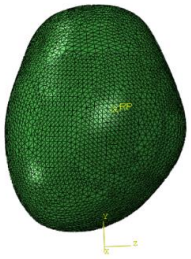

Fig. 2 Malha de EF obtida através do *morphing* para uma situação de plagiocefalia.

4 CONCLUSÃO

O algoritmo desenvolvido conseguiu realizar aquilo a que se propunha, com erros relativos percentuais relativamente reduzidos para os casos em que modificava apenas o tamanho da cabeça, e, para as craniossinostoses, com uma malha que qualitativamente demonstrava isso mesmo.

No futuro, o objetivo será simular o parto vaginal das diferentes cabeças criadas colocando a ventosa na posição considerada ideal e analisar se é a posição apropriada para cabeças fetais com morfologias incomuns.

AGRADECIMENTOS

Os autores agradecem o apoio da Fundação para a Ciência e a Tecnologia ao abrigo do Contrato de Investigador Júnior CEECIND/01522/2020, e o financiamento do Projeto UIDB/50022/2020.

REFERÊNCIAS

[1] A. Estevão, "Vacuum-Assisted Vaginal Delivery: a Biomechanical Study," Porto, Jul 2021.

[2], G. Tiago Pereira Roriz, "Parto computacional assistido," Master's Thesis, Faculdade de Engenharia da Universidade do Porto, Porto, 2015.

[3] C. Lourenco and J. Castro, "Vacuum delivery: A review of the literature." [Online]. Available: https://www.researchgate.net/publication/286103316

[4] Sofia Granja e Silva Teixeira Bernardo. In silico childbirth - towardshealthier mothers and offspring. Technical report, INEGI, 2022.

[5] R. Moura et al., "A numerical study on fetal head molding during labor," International Journal for Numerical Methods in Biomedical Engineering, vol. 37, no. 1, Jan. 2021, doi: 10.1002/cnm.3411

A.0.2 Article submitted for publication in a book of CNB papers in Springer's book series Lecture Notes in Bioengineering

Exploiting Technologies for Simulating Assisted Childbirth

Erica Ferreira[1] and Dulce Oliveira[2]

[1] FEUP, University of Porto. 4200-465 Porto, Portugal
[2] INEGI. 4200-465 Porto, Portugal
ericapf200@gmail.com

Abstract. Childbirth involves extensive physiological changes in the parturient to allow the passage of the fetus through the birth canal. In certain cases, there may be a need to perform an instrumented delivery, with the vacuum-cup being the instrument of choice since it minimizes the fetal trauma. Despite being a widely used practice, there are still uncertainties about the ideal place to positioning the vacuum-cup, especially when there are asymmetric heads. In this work, the morphing of several fetal head morphologies was performed using MATLAB for this purpose and ABAQUS to evaluate the morphing quality. The results obtained were used to simulate, using ABAQUS, and the Finite Element Method (FEM) methodology, the birth with and without a vacuum-cup, to evaluate the implications of the use of the vacuum-cup on the fetal head and on the maternal pelvis.

Keywords: Biomechanical Simulation, Craniosynostosis, Finite Element Methods, Morphing, Vaginal Delivery.

1 Introduction

1.1 Childbirth

Childbirth is a very complex natural and physiological process, which depends on the morphology and configuration of the maternal pelvis, as well as on uterine contractility and fetal size. Delivery corresponds to the sequence of events that result in the expulsion of the fetus and placenta through the vaginal canal at the end of pregnancy. During delivery, the fetal head is molded into an elongated shape as a result of external compressive forces and due to the presence of sutures and fontanelles and the elastic behavior of the skull bones [1,2]. When the course of labor is not favorable, it can be performed with the aid of instruments, as is the case of the vacuum-cup, which allows minimizing trauma to the fetus [3]. The correct placement of the vacuum-cup is crucial to ensure the success of the suction extraction process. Currently, there is an established flexion point on the fetal head that is ideal for the vacuum-cup placement, but this may not be appropriate for fetal heads with unusual morphologies. The implications of the vacuum-cup placement point on the fetal head and maternal muscles need to be

assessed. Computational models are valuable tools that allow the mechanisms of childbirth to be analyzed in a non-invasive way.

1.2 Craniosynostosis

When there is a premature fusion of one or more cranial sutures, we are faced with craniosynostosis. There are several types of craniosynostosis, as can be seen in the figure 1, however those explored in this project were scaphocephaly, which corresponds to the most frequent type of craniosynostosis, responsible for 40% to 60% of cases and is a consequence of the early closure of the sagittal suture. The plagiocephaly results from the early closure of one of the coronal sutures, which results in an oblique asymmetry of the head and the brachycephaly occurs due to the early closure of the coronal sutures, bilaterally. The skull has a short aspect, with an enlargement of the parietal bones and vertical growth [4,5].

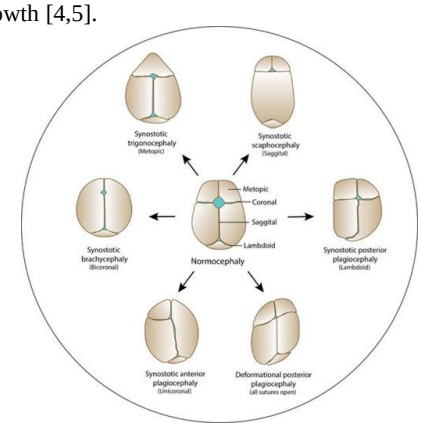

Fig. 1. Craniosynostosis and related sutures.

Thus, it is necessary to study the influence of the vacuum-cup on different types of heads, to understand its impact. To fulfill this goal, it is necessary to morph several fetal heads.

2 Methodology

2.1 Finite Elements Model

The fetal head finite element (FE) model used, which is represented in figure 2, from different perspectives, consists of the skin, sutures and fontanelles, skull, and brain and has 25459 nodes and 115762 elements [6].

The skin, skull and brain were modelled with solid tetrahedral elements. As the sutures and fontanelles correspond to the structures that allow the molding of the fetal head, their features should be as close as possible to reality. Therefore, they were modelled with membrane elements [6].

(a) (b) (c)

Fig. 2. FE model of the fetal head: (a) Frontal Plane, (b) Sagittal plane (bones highlighted) and (c) Transverse Plane (sutures highlighted).

The pelvic floor is composed of a group of muscles and fasciae in the female urogenital region. During pregnancy, together with the abdominal muscles, pelvic floor-muscles support the weight of the fetus, which generates an overload during the various months, making normal childbirth violent for these muscles [7].

The pelvic floor model used, shown in figure 3, was the one developed by Moura *et al.* in the study [6], having been modelled with a modified form of the transversely isotropic incompressible hyperplastic model proposed by Martins *et al.* [8] and the constitutive parameters were obtained from Parente *et al.* [9].

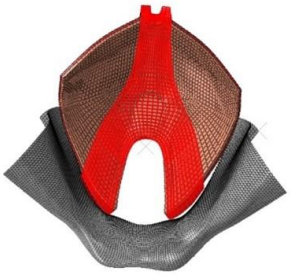

Fig. 3. FE model of the pelvis.

The model is composed of the pelvic floor muscles, represented in orange in figure 3, and the pubovisceral structure, represented in red, and these were modelled with hexahedral elements with hybrid formulation (C3D8H). The surface represented in grey (rigid quadrilateral shell elements) in figure 3 delimits the anterior region, imposing the limits that are anatomically ensured by the birth canal, replacing the anterior part of the pelvic bones. This surface allows the translation of the fetal head in the antero-posterior direction, ensuring a smooth contact surface between the fetal head and the replaced pelvic bones, improving the convergence of the simulations [6].

2.2 Morphing

To perform the morphing of the fetal head, the MATLAB software was used and Bernardo's algorithm [10] was adapted from the algorithm created by Moura *et al* [6], for each situation under study.

Regarding the diagnosis of plagiocephaly, the Plagiocephaly Index (PI) [11], presented in equation (1), can be used. It is obtained through the difference of the diagonals, which are represented in figure 4.

$$PI = D_1 - D_2 \quad (1)$$

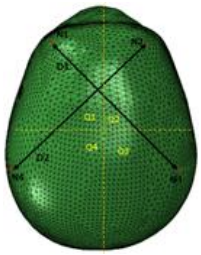

Fig. 4. Representation of the diameters used, and the nodes chosen.

In scaphocephaly and brachycephaly, the cephalic index [12], obtained through equation (2), changes according to the degree of severity.

$$IC = \frac{DBP}{DOF} \times 100 \quad (2)$$

As such, it was necessary to define the nodes that outline the diameters to be changed, as represented in the figure 5.

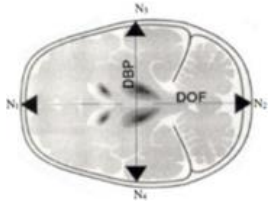

Fig. 5. Representation of the diameters used, and the nodes chosen.

For each craniosynostosis it was considered a deformation with moderate degree.

For the cases of conditions that only affect the size of the head, and not its shape, the altered diameters were the same as in the cases of scaphocephaly and brachycephaly.

After morphing was performed in MATLAB, the input files were run in ABAQUS to check whether morphing had occurred as intended. For the cases of plagiocephaly and scaphocephaly, the relative percentage error has a very low value, indicating that the diameters varied as expected. In the case of brachycephaly, despite the mesh

presenting the desired aspect, the morphing has a higher relative error, which indicates the need to optimize the algorithm for this situation.

To understand how the morphing performed on the mesh changed its quality, an analysis of the mesh quality was performed for each of the situations. For each situation, the elements with a weak shape (warnings) and the degenerated elements (errors) were determined and are presented in table 1.

Table 1. Mesh quality assessment.

	Plagiocephaly	Scaphocephaly	Brachycephaly
ϵ (%)	0,001%	0,003%	15,36%
Warnings	165 (0,142534%)	163 (0,140806%)	213 (0,183998%)
Errors	1 (0,00086%)	1 (0,00086%)	0

Considering the number of elements of each mesh, a high number of degenerated elements (errors) and elements with weak shape (warnings) was not obtained.

Next, the changes suffered by the sutures and fontanelles in each morphing were evaluated and are presented in table 2. These changes were evaluated in terms of fontanelles size, and it were considered, for the measurements, always the same points, that are presented in figures 6 and 7, where HF1 and HF2 correspond to the height of the anterior and posterior fontanelles respectively and CF1 and CF2 to their lengths.

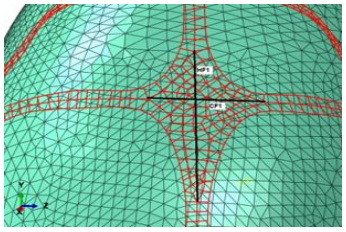

Fig. 6. Anterior Fontanelle.

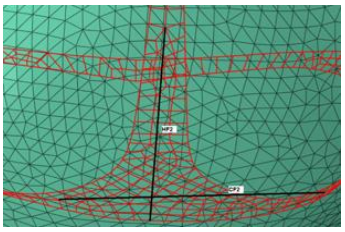

Fig. 7. Posterior Fontanelle.

Table 2. Results obtained for the fontanelles size.

Measurement (mm)	Normal	Scaphocephaly	Plagiocephaly	Brachycephaly
HF1	29,784	29,326	29,451	31,650
CF1	18,560	18,128	18,325	18,378
HF2	36,690	44,625	34,345	-
CF2	35,233	30,584	34,099	-

The size of the sutures decreased slightly in cases of plagiocephaly and scaphocephaly, while in brachycephaly, the size of the sutures involved increased considerably, which is not in accordance with what was expected, since in craniosynostosis there is early closure of the sutures, and their size should have decreased. As far as fontanelle size is concerned, in plagiocephaly and scaphocephaly the anterior fontanelle decreased in size, while in brachycephaly it increased in size. In brachycephaly the posterior fontanelle disappeared, and in the other two situations it underwent more modifications in terms of size when compared to the anterior fontanelle.

2.3 Biomechanical Simulations

The next step consisted of simulating the birth, firstly without a suction cup, and then using the scaphocephaly head for the continuation of the project.

Thus, using ABAQUS and a step-by-step approach, the simulation of the passage of the rigid head through the birth canal was performed. The first step consisted in aligning the head with the birth canal, and the subsequent steps consisted in lowering the head and adapting the maternal pelvis to this passage.

The simulations performed were adapted from the simulations carried out by Moura *et al.* [6], which were performed in Abaqus to mimic the second stage of labor, where the aim was to evaluate the consequences of delivering a fetus with scaphocephaly, without a suction cup, on the pelvic floor of the parturient woman. All movements of the fetal head are imposed by the reference node, which controls its translation and rotation during the different steps of the simulation, which starts with complete cervical dilation and ends with the passage of the head.

The standard Abaqus contact algorithm was used to impose the kinematic contact conditions, and contact constraints were established between the fetal head skin and the pelvic floor muscles, and between the fetal head skin and the pelvic bones. To create these conditions, a surface interaction with the Augmented Lagrange method was used.

Regarding the boundary conditions, the nodes corresponding to the ends of the pelvic floor muscles, the pubic bone and the pelvic fascia connecting to the pelvic bone were fixed.

About the duration of labor, in nulliparous women (who have never had a birth) the average duration of the second stage is highly variable [13]. The normal duration of a labor is between 30 min and 180 min [14]. If the duration is shorter or longer, it is a

precipitate or prolonged birth, respectively. In the simulations performed a delivery was simulated with a duration of 100 min.

3 Results

At first the stretch suffered by the maternal pelvis was evaluated considering the vertical displacement suffered by the fetal head. According to Lien et al. a stretch above 1.5 may indicate that the muscles have suffered considerable damage. In this study, a maximum stretch of 1.93 was obtained, corresponding to a vertical displacement of 65 mm, indicating that in this case the muscles of the maternal pelvis probably suffered considerable damage. Comparing these results with those obtained in the study carried out by Moura *et al.* [6] there was an increase of approximately 31.82% in the stretch, as it is shown in figure 8.

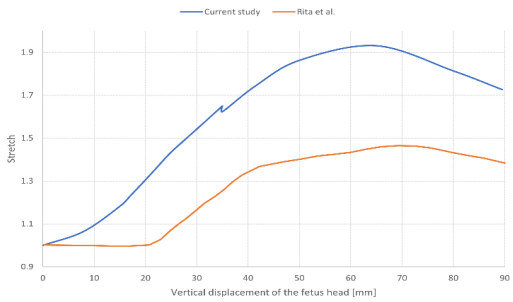

Fig. 8. Stretch calculated along the normalized trajectory in the lowest portion of the pelvic floor.

Next, the maximum principal Cauchy stresses were analyzed for two key moments of the simulation: its end and the maximum stretch moment. As we can see in figure 9 for the moment of maximum stretch, we have a maximum stress of about 15.69 MPa, while in the end of the simulation a maximum stress of 1.920MPa, as it's shown in figure 10.

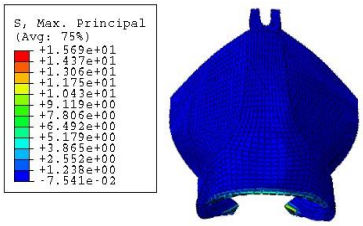

Fig. 9. Distribution of maximum principal Cauchy tensions (MPa) in the pelvic floor muscles for the moment of maximum stretch.

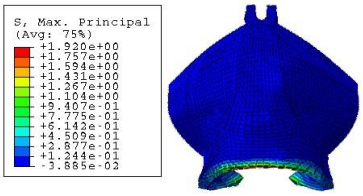

Fig. 10. Distribution of maximum principal Cauchy tensions (MPa) in the pelvic floor muscles at the end of the simulation.

Figure 11 have the maximum principal Cauchy stresses in relation to the normalized distance along the path for the moment when we have the maximum stretch. It is important to mention that this path is the same one that was used to obtain the stretch values.

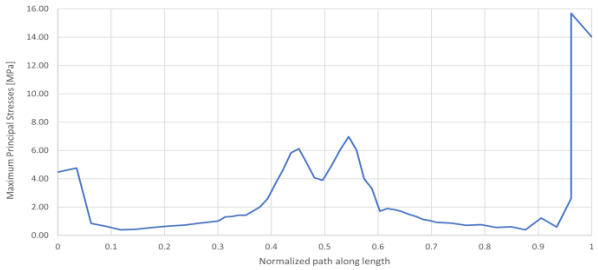

Fig. 11. Maximum principal Cauchy stresses (MPa) on the pelvic floor muscles for the maximum stretch instant.

Finally, the reaction forces were analyzed in relation to the vertical displacement, and their magnitude is represented in figure 12.

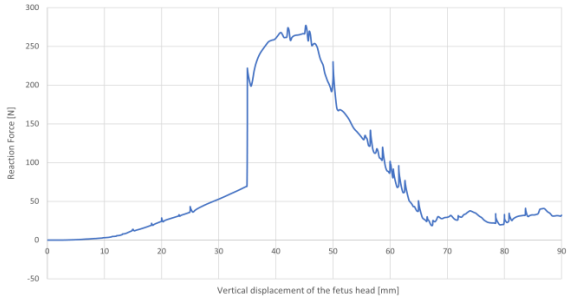

Fig. 12. Reaction forces in relation to vertical displacement.

Compared with the study performed by Moura *et al.* [6] the forces obtained were about 10 times higher, however the model of the pelvis used was not the same, in this study the fetal head used was a rigid body, while in the other one it was a moldable head.

4 Conclusion

The simulation of biological processes has emerged in the field of Medicine, as a complement to case studies and the development of therapies and improvement of conventional procedures. Childbirth comprises a complex and unpredictable mechanism, and the methodologies used in this process are applicable to the general population, but in more unusual cases they may have severe consequences. The use of a suction cup in assisted childbirth minimizes trauma to the fetus at birth, however, if placed in the wrong position, it may injure and cause harm to the newborn and the mother. In fact, the ideal position of the suction cup is defined for the great majority of heads, however, for heads with more unusual shapes, the adoption of the same position may not be the most correct practice. Thus, it is important to study the deformation that the various types of heads undergo through the suction cup. To this end, biomechanical simulation is a key tool.

In this study, the stretch obtained may indicate the presence of considerable lesions in the maternal pelvis, and considerably higher reaction forces were obtained when compared to previous studies.

Currently, the simulation with the suction cup has already been carried out to study its influence, and the results are being analyzed.

In terms of future work, it would be interesting to repeat the study, but for other head shapes, and, furthermore, for a deformable head. Besides, it would be interesting to perform the simulation for different positions and formats of the suction cup.

References

1. Estevão, A.: Vacuum-Assisted Vaginal Delivery: a Biomechanical Study. Porto (2021).
2. Roriz, G.: Parto Computacional Assistido. Porto (2015).
3. Lourenço, C., Castro, J.: Vacuum delivery: A review of the literature, https://www.researchgate.net/publication/286103316, last accessed 2023/02/01.
4. Oliveira, M., Marcelino, J.: Craniossinostoses - desenvolvimentos recentes. Coimbra.
5. Ghizoni, E. *et al.*: Diagnóstico das deformidades cranianas sinostóticas e não sinostóticas em bebês: uma revisão para pediatras. Revista Paulista de Pediatria 34(4), 495-502 (2016).
6. Moura, R., *et al.*: A numerical study on fetal head molding during labor. International Journal for Numerical Methods in Biomedical Engineering 37(1), (2020).
7. Silva, M.: Estudo biomecânico de um feto durante um parto vaginal. Porto (2012).
8. Martins, J., Pires, E., Salvado, R.: A numerical model of passive and active behavior of skeletal muscles. Comput Methods Appl Mech Eng. 151(3-4), 419–433 (1998).
9. Parente, M., Natal, R.: The influence of the material properties on the biomechanical behavior of the pelvic floor muscles during vaginal delivery. J. Biomech. 42(9), 1301–1306 (2009).

10. Bernardo, S.: In silico childbirth – towards healthier mothers and offspring. Porto (2022).
11. Joan, B., Josep, C.: Plagiocefalia posicional: uma tarefa de escola primária. Directrizes para diagnóstico, prevenção, acompanhamento e encaminhamento a partir dos cuidados primário. EAP Rambla (ICS). Sant Feliu de Llobregat.
12. Melo, J.: Craniossinostoses. Revista brasileira de Neurologia e Psiquiatria 18(2), 110–112 (2014).
13. Leveno, KJ.: Williams ObstetricsMcGraw-Hill Education 25. New York (2018).
14. Hoffman MK., Quiñones JN., Gómez D.: Length of the second stage of labor and preterm delivery risk in the subsequent pregnancy. Am J Obstet Gynecol 219(5). (2018).

A.0.3 Abstract submitted at the Young Research Meeting of the University of Porto (IJUP)

Exploring technologies for simulating assisted childbirth

Erica Ferreira, FEUP, Portugal
Dulce Oliveira, INEGI, Portugal

Abstract

Parturition is a natural and highly complex physiological process influenced by fetal size. Sometimes it can be accomplished with the assistance of instruments, like the vacuum-cup. However, for this process to succeed, the vacuum-cup must be correctly positioned [1]. There is currently a defined point where it should be placed, yet there are various head formats and sizes, so the point considered ideal for a standard head may not be appropriate for an asymmetric one. This project aimed to create different fetal heads with asymmetries (craniosynostoses) to then simulate the impact of the vacuum-cup on the maternal pelvis. It was used MATLAB to create an algorithm that allowed the morphing for each craniosynostosis. To ensure that the morphed head is suitable for simulation purposes, an analysis was performed on the new meshes created in ABAQUS. This analysis can help identify any potential problems with the new geometry, like areas of high stress concentration or with insufficient mesh resolution. Qualitatively all heads presented the desired shape, still the morphing had a high relative error for brachycephaly. In general, the meshes had a good quality and the elements did not deviate much from their ideal shape. The size of the sutures and fontanelles was also evaluated, having decreased in the situations of plagiocephaly and scaphocephaly. In brachycephaly, the size of the sutures and anterior fontanelle increased, and the posterior fontanelle disappeared, contrary to what was expected.

Keywords: Craniosynostosis, Finite Element Method, Computational Modelling, Morphing.

Acknowledgments

The authors gratefully acknowledge support from the Foundation for Science and Technology under the Junior Researcher Contract CEECIND/01522/2020, and funding from Project UIDB/50022/2020.

References

[1]A. Estevão, "Vacuum-Assisted Vaginal Delivery: a Biomechanical Study," Porto, Jul 2021.

A.0.4 Abstract submitted to the 28th Congress of the European Society of Biomechanics (ESB)

SUCTION CUP PLACEMENT IN INSTRUMENTED VAGINAL DELIVERY

Dulce Oliveira (1), Erica Ferreira (2)

1. INEGI, LAETA & FEUP, Portugal; 2. FEUP, Portugal

Introduction

Delivery is a very complex natural and physiological process, which depends on the morphology and configuration of the maternal pelvis as well as uterine contractility and fetal size [1]. When the course of labor is not favorable, it can be performed with the help of instruments, such as the suction cup, which allows minimizing trauma to the fetus. The correct placement of the suction cup is crucial to ensure the success of the suction cup extraction process. Currently, there is an established flexion point on the fetal head that is ideal for suction cup placement, but this may not be appropriate for fetal heads with unusual morphologies. The implications of the suction cup placement point on the fetal head and maternal muscles need to be evaluated. Computational models are valuable tools that allow the analysis of the mechanisms of childbirth in a non-invasive way.

Methods

The morphing of several fetal head morphologies was performed in order to simulate the impact of instrumented delivery on the maternal pelvis. For this purpose, MATLAB was used, and an algorithm was adapted that allowed morphing these structures, based on the finite element model of a standard fetal head, which is shown in Figure 1.

a. b.

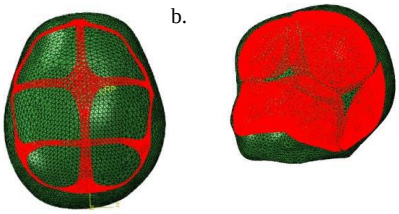

Figure 1: Fetal head FE model used. In red are (a.) sutures and (b.) bones.

In addition to morphing for several percentiles, including prematurity and macrocephaly, morphing was also performed for situations that introduced asymmetries in the head (craniosynostosis). To ensure the success of the morphing, the ABAQUS software was used.

The methodology chosen for morphing the fetal head for different percentiles included defining the biparietal diameter (BPD) and occipitofrontal diameter (OFD) and establishing their relationship with the cephalic perimeter. In the case of craniosynostosis, it was necessary to establish other diameters and relationships between them, to cause the desired deformation.

Results

Figure 2 the morphing results for each of the craniosynostoses in study.

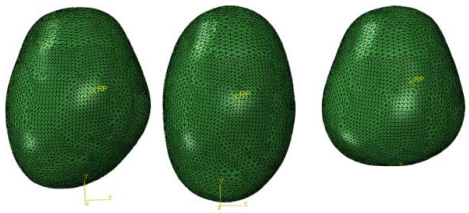

a. plagiocephaly b. scaphocephaly c. brachycephaly

Figure 2: FE mesh obtained after morphing for each of the craniosynostoses in study.

To understand how the morphing performed on the mesh changed its quality, a mesh quality analysis was performed (Figure 3).

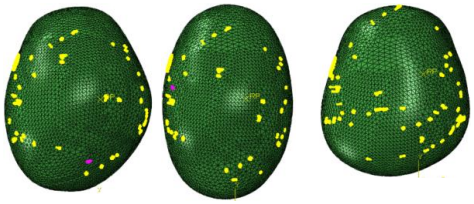

a. plagiocephaly b. scaphocephaly c. brachycephaly

Figure 3: Quantification of the distortion of the elements, where in yellow are the warnings and the pink ones the errors.

Discussion

The developed algorithm achieved the proposed objectives, with relatively low percentage relative errors and with meshes with good quality. In the future, the goal will be to simulate the vaginal delivery of the different heads created by placing the suction cup in the position considered ideal and analyze if it is the appropriate position for fetal heads with unusual morphologies.

References

1. Estevão, "Vacuum-Assisted Vaginal Delivery: a Biomechanical Study," MSc Thesis, Porto, 2021.

Acknowledgements

The authors are grateful for the support of FCT under the Junior Researcher Contract CEECIND/01522/2020, and the funding from Project UIDB/50022/2020.

References

[1] Rita Moura, Margarida Borges, Maria Vila Pouca, Dulce Oliveira, Marco Parente, Nina Kimmich, Teresa Mascarenhas, and Renato Natal. A numerical study on fetal head molding during labor. *International Journal for Numerical Methods in Biomedical Engineering*, 37(1), October 2020.

[2] Helen Feltovitch. Labour and delivery: a clinician's perspective on a biomechanics problem. *Interface Focus*, 2(9), July 2019.

[3] Barbara Nolens, Thomas van den Akker, John Lule, Sulphine Twinomuhangi, Jos van Roosmalen, and Josaphat Byamugisha. Women's recommendations: vacuum extraction or caesarean section for prolonged second stage of labour, a prospective cohort study in uganda. *Tropical Medicine and International Health*, 24(5):553–562, May 2019.

[4] Hoffman MK. Quiñones JN, Gómez D. Length of the second stage of labor and preterm delivery risk in the subsequent pregnancy. *Am J Obstet Gynecol*, 219(5), 2018.

[5] PE Bailey, J van Roosmalen, G Mola, C Evans, L de Bernis, and B Dao. Assisted vaginal delivery in low and middle income countries: an overview. *BJOG*, 124:1335–1344, January 2017.

[6] Rudy Lapeer, Zelimkhan Gerikhanov, and Vilius Audinis. A computer-based simulation of vacuum extraction during childbirth. November 2014. SIMULIA Regional User Meeting RUM 2014 ; Conference date: 04-11-2014 Through 05-11-2014.

[7] J.-P. Schaal, V. Equy, and P. Hoffman. Comparaison ventouse forceps. *Journal de Gynécologie Obstétrique et Biologie de la Reproduction*, 37(8, Supplement 1):S231–S243, 2008. Recommandations pour la pratique clinique.

[8] DJ Murphy, BK Strachan, and R Bahl. Assisted vaginal birth. *BJOG*, 127:70–112, April 2020.

[9] Cátia Lourenço, Joana Silva, Jorge Castro, Mariana Veiga, and Claudina Carvalho. Ventosa obstétrica: Uma revisão da literatura. *Arquivos de Medicina*, 26(6):254–263, 2012.

[10] Frédérik Michas. Porcentagem de nascimentos entregues por fórceps ou extração a vácuo nos estados unidos de 1990 a 2020, Maio 2022. Available in https://www.statista.com/statistics/276067/us-births-delivered-by-forceps-or-vacuum-extraction/#statisticContainer. Accessed in October 2022.

[11] Hartmut Bossel. *Modeling and Simulation*. A K Peters/CRC Press, 1st edition, 1994.

[12] Ana Estevão. Vacuum-assisted vaginal delivery: a biomechanical study. Master's dissertation, July 2021. Faculdade de Engenharia da Universidade do Porto.

[13] Gaspar Roriz. Parto computacional assistido. Master's dissertation, February 2015. Faculdade de Engenharia da Universidade do Porto.

[14] Academia PNA. *Mecanismos do Parto Normal*. Manual APNA - Ginecologia e obstetrícia. Available in https://www.academiapna.com. Accessed in November 2022.

[15] Marco Parente. *Biomechanics of the Pelvic Floor during Vaginal delivery*. Doctoral thesis, June 2008. Faculdade de Engenharia da Universidade do Porto.

[16] Enrico Ghizoni, Rafael Denadai, Cesar Augusto Raposo-Amaral, Andrei Fernandes Joaquima, Helder Tedeschi, and Cassio Eduardo Raposo-Amaral. Diagnóstico das deformidades cranianas sinostóticas e não sinostóticas em bebês: uma revisão para pediatras. *Revista Paulista de Pediatria*, 34(4):495–502, May 2016.

[17] Manuel António da Silva Oliveira and João Pedro Marcelino. Craniossinostoses - desenvolvimentos recentes. Technical report, Faculdade de Medicina da Universidade de Coimbra.

[18] Swya Oliveira Xavier. Deformidade craniana do recém-nascido prematuro: Implicações para a equipe de enfermagem. Master's dissertation, December 2011. Universidade Federal do Estado do Rio de Janeiro.

[19] Enfermagem Online. Fontanelas e suturas cranianas dos recém-nascidos, February 2015. Available in https://enfermagemonlinebr.wordpress.com/2015/02/06/fontanelas-e-suturas-cranianas-dos-recem-nascidos/. Accessed in October 2022.

[20] Studypool. Stages phases of labor, September 2021. Available in https://www.studypool.com/documents/4593156/stages-phases-of-labor. Accessed in November 2022.

[21] Catia Lourenco, J. Silva, Jorge Castro, M. Veiga, and C. Carvalho. Vacuum delivery: A review of the literature. *Arquivos de Medicina*, 26:254–263, 11 2012.

[22] Direcção-Geral da Saúde. Consultas de vigilância de saúde infantil e juvenil - atualização das curvas de crescimento, February 2006. Available in https://www.dcc.fc.up.pt/~ines/aulas/1516/DM1/UCMF-explanations-and-tables/imc_sandra.pdf. Accessed in September 2022.

[23] Phyllis Zelkowitz. Prematuridade e seu impacto sobre o desenvolvimento psicossocial e emocional da criança. Technical report, McGill University, April 2017.

[24] 0 Guayasamín, W. L. Benedetti, 0 Althabe, F. Nieto, , and S. Tenzer. Crescimento fetal humano valorado por indicadores antropometricos. *Boletin de la Oficina Sanitaria Panamericana*, December 1976.

[25] M. Rosado annd M. Barbieri, H. Bettiol, U. A. Gomes, and V. Ribeiro. Crescimento craniano na criança. *Arq Neuro-Psiquiat*, 4(47), 1989.

[26] L. Yaned, G. Bejarano, F. H. Tejedor, L. Alberto, L. Pérez, , and C. I. Contreras. Head circumference growth curves in children 0 to 3 years of age. a new approach. *Rev Fac Odontol Univ Antioq*, 26(1):13–32, 2014.

[27] E.-R. Jal, L.-C. WA, I.-L. J, and B.-Z. I. Changes in weight, length and head circumference in very low birth weight new born during their stay in the unit neonatal intensive care and the relationship with reference pattern. *Sanid Milit*, 2016.

[28] C Geoffrey Woods. Human microcephaly. *Current Opinion in Neurobiology*, 14:112–117, 2004.

[29] Manual MSD. Percentis de perímetro cefálico de bebês para a idade, segundo a oms (<24 meses), 2022. Available in https://www.msdmanuals.com/pt-pt/profissional/multimedia/clinical-calculator/percentis-da-oms-do-per%C3%ADmetro-cef%C3%A1lico-por-idade-para-rec%C3%A9m-nascidos-24-meses. Acessed in October 2022.

[30] Mónica Vilarinho Andersen. Cranioplastia de redução assistida por modelo 3d para macrocefalia extrema e plagiocefalia secundárias a hidrocefalia não tratada - caso clínico. Master's dissertation, July 2021. Faculdade de Medicina da Universidade de Lisboa.

[31] José Aloysio Costa Val Filho. As medidas cranianas no diagnóstico das craniossinostoses. Master's dissertation, November 2013. Faculdade de Medicina da UFMG.

[32] José Roberto Tude Melo. Craniossinostoses. *Revista brasileira de Neurologia e Psiquiatria*, 18(2):110–112, August 2014.

[33] Edward Buchanan, Yunfeng Xue, Amy Xue, Asaf Olshinka, and Sandi Lam. Multidisciplinary care of craniosynostosis. *Journal of Multidisciplinary Healthcare*, 10:263–270, 07 2017.

[34] Joan Bosch i Hugas and Josep Maria Costa i Clara. Plagiocefalia posicional: uma tarefa de escola primária.directrizes para diagnóstico, prevenção, acompanhamento e encaminhamento a partir dos cuidados primários. Technical report, EAP Rambla (ICS), Sant Feliu de Llobregat.

[35] Danish Mohammad and Sivashanmugam Dhandapani. Trigonocephaly: A simple modified technique. *J Pediatr Neurosci.*, 9(2):125–128, May 2014.

[36] Ricardo J. Fernández de Thomas; Orlando De Jesus. Trigonocephaly. *StatPearls [Internet]*, November 2022. Available in https://www.ncbi.nlm.nih.gov/books/NBK565874/. Accessed in November 2022.

[37] Paul A. Riemenschneider. Trigonocephaly. *Radiology*, 68(6):863–865, 1957. PMID: 13441914.

[38] Sergio Silva, João Medeiros, and Rebeca Aelncar. Um caso de craniosinostose da sutura sagital em um subadulto do sítio arqueológico furna do nego, município de jataúba, pernambuco, brasil. Technical report, Universidade Federal de Pernambuco, 2015.

[39] Renato da Silva Freitas, Nivaldo Alonso, Joseph H. Shin, and John Persing. Assimetrias cranianas em crianças: diagnóstico diferencial e tratamento. *Rev Bras Cir Craniomaxilofac*, 13(1):44–48, 2010.

[40] Hiroshi Miyabayashi, Nobuhiko Nagano, Risa Kato, Takanori Noto, Shin Hashimoto, Katsuya Saito, and Ichiro Morioka. Cranial shape in infants aged one month can predict

the severity of deformational plagiocephaly at the age of six months. *Journal of Clinical Medicine*, 11, March 2022.

[41] Sorbe B and Dahlgren S. Some important factors in the molding of the fetal head during vaginal delivery - a photographic study. *Int J Gynecol Obstet*, 21(3):205–212, 1983.

[42] M. G. Pandy. Computer modeling and simulation of human movement, 2001. Available in http://www.annualreviews.org. Accessed in November 2022.

[43] Daniel Sieger, Stefan Menzel, and Mario Botsch. High quality mesh morphing using triharmonic radial basis functions. In Xiangmin Jiao and Jean-Christophe Weill, editors, *Proceedings of the 21st International Meshing Roundtable*, pages 1–15, Berlin, Heidelberg, 2013. Springer Berlin Heidelberg.

[44] Ian A Sigal, Michael R Hardisty, and Cari M Whyne. Mesh-morphing algorithms for specimen-specific finite element modeling. *J Biomech*, 41(7):1381–1389, April 2008.

[45] Aaron W. F. Lee, David Dobkin, Wim Sweldens, and Peter Schr¨oder. Multiresolution mesh morphing. Technical report, Princeton University, 1999.

[46] Computational modeling [Internet]. Mesh-morphing techniques. Available in https://computationalmodeling.info/. Accessed in January 2023.

[47] R.J. Lapeer and R.W. Prager. Fetal head moulding: finite element analysis of a fetal skull subjected to uterine pressures during the first stage of labour. *Journal of Biomechanics*, 34:1125–1133, April 2001.

[48] Mathieu Bailet, Florence Zara, and Emmanuel Promayon. Biomechanical model of the fetal head for interactive childbirth simulation. *SURGETICA*, pages 116–119, December 2014.

[49] Fang Pu, Liqiang Xu, Deyu Li, Shuyu Li, Lianwen Sun, Ling Wang, and Yubo Fan. Effect of different labor forces on fetal skull molding. *Medical Engineering Physics*, 33:620–625, 2011.

[50] M.E.T. Silva, D.A. Oliveira, T.H. Roza, S. Brandão, M.P.L. Parente, T. Mascarenhas, and R.M. Natal Jorge. Study on the influence of the fetus head molding on the biomechanical behavior of the pelvic floor muscles, during vaginal delivery. *Journal of Biomechanics*, 48(9):1600–1605, 2015. Reproductive Biomechanics.

[51] Dejun Jing, James A Ashton-Miller, and John O L DeLancey. A subject-specific anisotropic visco-hyperelastic finite element model of female pelvic floor stress and strain during the second stage of labor. *Journal of biomechanics*, 45(3):455—460, February 2012.

[52] Rongrong Xuan, Mingshuwen Yang, Yajie Gao, Shuaijun Ren, Jialin Li, Zhenglun Yang, Yang Song, Xu-Hao Huang, Ee-Chon Teo, Jue Zhu, and Yaodong Gu. A simulation analysis of maternal pelvic floor muscle. *International journal of environmental research and public health*, 18(20):254–263, 10 2021.

[53] Chuang-Yen Huang, Kuo-Min Su, Hsueh-Hsing Pan, Fung-Wei Chang, Yu-Ju Lai, Hung-Chih Chang, Yu-Chi Chen, Chi-Kang Lin, and Kuo-Chih Su. Investigating the effects of different sizes of silicone rubber vacuum extractors during the course of delivery on the fetal head: A finite element analysis study. *Polymers*, 14(4), 2022.

[54] Yu-Hsuan Chen, Kuo-Min Su, Ming-Tzu Tsai, Chi-Kang Lin, Cheng-Chang Chang, and Kuo-Chih Su. Investigating the vacuum extractors of biomedical devices of different materials and pressures on the fetal head during delivery. *Applied Sciences*, 11(17), 2021.

[55] J. Fish and T. Belytschko. A first course in finite elements. Technical report, 2007.

[56] Sofia Granja e Silva Teixeira Bernardo. In silico childbirth - towardshealthier mothers and offspring. Technical report, INEGI, 2022.

[57] Mathworks [Internet]. Matlab, 2022. Available in www.mathworks.com. Accessed in December 2022.

[58] W. Lin. 3d point set warping by thin-plate/rbf function, 2022. Available in *MATLAB Central File Exchange*. Accessed in December 2022.

[59] Sérgio Wagner Fragoso Stachinski. Diâmetro biparietal- valores normais ig (semanas) relações biométricas fetais, 2019. Available in https://docplayer.com.br/. Accessed in November 2022.

[60] M. Fujita, M. Okumura, J. Singer, D. Andrade, and M. Zugaib. Curva de crescimento do diâmetro biparietal e da circunferência. *RBGO*, 21(10), 1999.

[61] Gerd Schreen and Carolina Gomes Matarazzo. Tratamento de plagiocefalia e braquicefalia posicionais com órtese craniana: estudo de caso. *Einstein*, 11(1):114–118, 2013.

[62] 4RealSim. Mesh quality checks tools abaqus, 2020. Available in https://www.4realsim.com/mesh-quality-checks-tools-abaqus/. Accessed in January 2023.

[63] SIMULLIA. Verifying your mesh. Available in https://classes.engineering.wustl.edu/2009/spring/mase5513/abaqus/docs/v6.6/books/usi/default.htm?startat=pt03ch17s06s01.html. Accessed in January 2023.

[64] Maria Elisabete Teixeira Silva. Estudo biomecânico de um feto durante um parto vaginal. Master's dissertation, July 2012. Faculdade de Engenharia da Universidade do Porto.

[65] Martins JAC, Pires EB, and Salvado R. A numerical model of passive and active behavior of skeletal muscles. *Comput Methods Appl Mech Eng.*, 151(3-4):419–433, 1998.

[66] Marco Parente and Renato Natal. The influence of the material properties on the biomechanical behavior of the pelvic floor muscles during vaginal delivery. *J. Biomech*, 42(9):1301–1306, 2009.

[67] Gimovsky ML O'Grady PJ and McIlhargie CJ. Vacuum extraction. *Modern Obstetric Practice*, 63, 1995.

[68] Leveno KJ. *Williams Obstetrics*. New York: McGraw-Hill Education, 25th edition, 2018.

[69] Mooney B. Lien K. Levator ani muscle stretch induced by simulated vaginal birth. *Obstet Gynecol*, 103(1):31–40, 2004.

[70] Rupinder Singh and S. Singh. Additive manufacturing: An overview. In Abdul-Ghani Olabi, editor, *Encyclopedia of Smart Materials*, pages 258–269. Elsevier, Oxford, 2017.

[71] Stavropoulos P. Chryssolouris G. Bikas, H. Additive manufacturing methods and modelling approaches: a critical review. *Int J Adv Manuf Technol*, 83:389–405, 2016.

[72] B. Vayre, F. Vignat, and F. Villeneuve. Designing for additive manufacturing. *Procedia CIRP*, 3:632–637, 2012. 45th CIRP Conference on Manufacturing Systems 2012.

[73] 3DLAB. Pla: tudo o que você precisa saber sobre o filamento pla. Available in https://3dlab.com.br/pla-tudo-o-que-voce-precisa-saber-sobre-o-filamento-pla/. Accessed in May 2023.

[74] I. John Solomon, P. Sevvel, and J. Gunasekaran. A review on the various processing parameters in fdm. *Materials Today: Proceedings*, 37:509–514, 2021. International Conference on Newer Trends and Innovation in Mechanical Engineering: Materials Science.

[75] Kaufui V. Wong and Aldo Hernandez. A review of additive manufacturing. *ISRN Mechanical Engineering*, 2012.

[76] Valentina Mazzanti, Lorenzo Malagutti, and Francesco Mollica. Fdm 3d printing of polymers containing natural fillers: A review of their mechanical properties. *Polymers*, 11(7), 2019.

[77] Miguel de Abreu Paramos de Carvalho. Conception and development of a feeding system for fdm machines. Technical report, Técnico Lisboa, December 2018.

[78] esun. Water washable resin. Available in https://www.esun3d.com/water-washable-resin-product/. Accessed in June 2023.

[79] sculpteo. Lcd and dlp 3d printing technologies. Available in https://www.sculpteo.com/en/materials/lcd-dlp-technologies/. Accessed in June 2023.